POLITECNICO DI TORINO
Repository ISTITUZIONALE

Mathematical modelling of the loss of tissue compression responsiveness and its role in solid tumour development

(Article begins on next page)

13 July 2024

Mathematical Modelling of the Loss of Tissue Compression Responsiveness and its Role in Solid Tumour Development

*M.A.J. Chaplain, **L. Graziano, **L. Preziosi

November 7, 2005

* Department of Mathematics — University of Dundee
chaplain@maths.dundee.ac.uk

** Department of Mathematics — Polytechnic of Turin
luigi.graziano@polito.it - luigi.preziosi@polito.it

Abstract

This paper presents a mathematical model of normal and abnormal tissue growth. The modelling focuses on the potential role that stress responsiveness may play in causing proliferative disorders which are at the basis of the development of avascular tumours. In particular, we study how an incorrect sensing of its compression state by a cell population can represent a clonal advantage and can generate hyperplasia and tumour growth with well known characteristics such as compression of the tissue, structural changes in the extracellular matrix, change in the percentage of cell type (normal or abnormal), extracellular matrix and extracellular liquid. A spatially independent description of the phenomenon is given initially by a system of nonlinear ordinary differential equations which is explicitly solved in some cases of biological interest showing a first phase in which some abnormal cells simply replace the normal ones, a second phase in which the hyper-proliferation of the abnormal cells causes a progressive compression within the tissue itself, and a third phase in which the tissue reaches a compressed state, which presses on the surrounding environment. A travelling wave analysis is also performed which gives an estimate of the velocity of the growing mass.

1 Introduction

Over the last few years there has been a lot of attention paid to modelling avascular tumour growth and tumour invasion of host tissue, as can be seen from the books [1, 90], the special issues [9, 12, 29, 30] specifically devoted to these topics, and the references therein. Most of the modelling carried out in these papers starts from the observation that tumour cells become insensitive to anti-growth signals and evade apoptosis. Having lost their internal programme-for-cell-death, they acquire a limitless replicative potential, grow rapidly and invade the surrounding tissue (see [9, 13] and [31] for recent reviews). Attention is then focussed on how the nutrient (e.g., oxygen) diffusing through the tumour boundary affects the growth of the tumour, with the formation of a necrotic core, of an intermediate layer of quiescent cells and an outer rim of proliferating cells. Most mathematical models are characterised by the existence of a limiting radius, as is well-known from experiments [46, 103].

In this paper we start from a different point of view and examine certain important biomechanical factors. Specifically, we focus on the role of how a cell senses the presence of other cells and its own compression state, how this affects its proliferative ability and how an imperfect perception may cause hyperplasia, which here is considered as an early event of tumorigenesis. Thus for the purposes of our model, we neglect the effects of external nutrients and other chemical/growth factors and choose to focus solely on biomechanical effects.

As will be discussed in the following section which will focus on the description of the experimental evidences, several papers have studied the effect of stress on the process of mitosis and apoptosis of tumour cells. In order to deal with growing biological tissues, recently the concepts of multiple natural configuration and of accretive forces have been introduced to model tissues as continua which continuously remodel while undergoing large

1

deformations [3, 4, 5, 43, 48, 61, 94]. In fact, the simultaneous presence of growth and deformation make it impossible to use standard continuum mechanics. This approach was used by Ambrosi and Mollica [6] to model the growth in vitro of a multicellular spheroid in gels of variable stiffness obtaining results in good qualitative agreement with the experiment by Helmlinger et al. [57].

On the other hand, to take into account the different constituents present in a tumour, the use of the theory of mixtures was proposed in [23]. This approach also enables the stresses within the tumour to be evaluated. The link between the model proposed here and the one in [23] consists in the inclusion of the dependence of the cell proliferation rate on the cellular stress. Many other applications of multiphase models have been proposed in [7, 17, 18, 19, 22, 45, 91], some of them also including the effect of the mechanical interactions with the sorrounding tissues.

The main aim of this paper is to show how an underestimation of the compression state of the local tissue and then of the subsequent stress which is exerted on a cell, can generate by itself a clonal advantage on the surrounding cells leading to the replacement and the invasion of the healthy tissue.

In addition to biomechanical effects, the model also takes into account the effect of the production of extracellular matrix (ECM) and of matrix degrading enzymes (MDEs). In fact, cells produce extracellular matrix which is important for cell adhesion, spreading and motility. Therefore, on the one hand the extracellular matrix may constitute a barrier to normal cell movement, and on the other hand it provides a substratum cells may use to adhere and move. Most mammalian cell types require at least some elements of the extracellular matrix to be present for growth and survival and will indeed migrate up a gradient of bound (i.e. non-diffusible) cell adhesion molecules in culture *in vitro* [24, 68, 69, 71, 80, 93].

On the other hand, matrix degrading enzymes are also important at many stages of tumour growth, invasion and metastasis, and the manner in which they interact with inhibitors, growth factors and tumour cells is very complex. However, it is well known that tumour cells produce matrix degrading enzymes which degrade the extracellular matrix.

In summary, we start from the assumption that when cells are in a crowded environment they sense the presence of other cells and their behaviour then crucially depends on how they can stand the pressure. We then focus on how this can affect both mitosis and production of extracellular matrix and matrix degrading enzymes. We start from the following phenomenological observations which are described with further detail in the following section:

- Cells replicate if they sense there is sufficient space to accomplish this. If, on the other hand, they sense that there is a sufficient number of cells around them, they can alter their activity and enter a quiescent state ready to re-activate their replication programme if, for instance, a neighbouring cell dies;

- Cells constantly produce ECM and matrix degrading enzymes;

- Cells move preferentially toward regions with lower stress.

Of course, we are well aware that cellular mechanotrasduction is not the only cause of formation of hyperplasia and tumours and that chemical factors will operate to regulate the reproduction rates. However, in this paper we want to focus specifically on the role of cell contact and compression. In fact, we assume that the only thing that changes a normal cell into an abnormal (transformed) cell is how it senses and responds to the stress exerted on it. If a cell does not sense stress correctly, it continues to replicate even when there are already other cells around it and insufficient space for the daughter cells. This gives rise to hyperplasia and tumours in the local tissue. In this paper then the stress and therefore its influence on the evolution of the cell population occurs through three contributions: cell replication, the production of extracellular matrix and the release of matrix degrading enzymes.

The paper is laid out as follows. The following section is devoted to a detailed description of the biological aspects covered by the model deduced in Section 3. We then study in Section 4 the properties of the model starting from the simplest version and then including more complicated effects along the way, giving analytic solutions and qualitative behaviours whenever possible. More precisely, Section 4.1 describes how the model is able to describe the generation of confluent distributions in vitro in view of the identification of some parameters. Section 4.2 focuses on the re-construction of a normal healthy tissue with matrix degrading enzymes controlling the content of extracellular matrix and allowing a continuous renewal of extracellular matrix. Section 4.3 describes how the occurrence of a genetic change in a cell causing only an inadequate sensing of stress which affects only cell replication, can lead to the complete replacement of the healthy tissue and to an overcompression
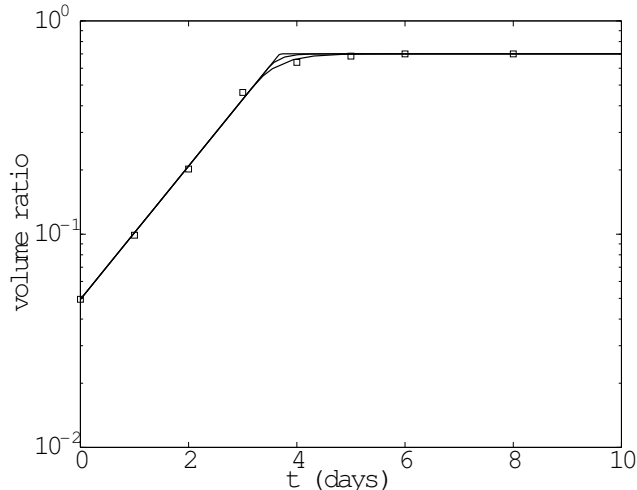
Figure 1: Growth of human breast epithelial cells. The squares refer to the experimental results by Tsukatani et al. [107], the lines to the simulation obtained using the model (14) solved by (15) for the duplication time given there (22.3 days) and for different values of σ. From above to below $\sigma = 0.01, 0.1, 0.2$.

of the tissue. In particular, the normal extracellular matrix is completely replaced by the tumour-generated matrix. Section 4.4 describes what happens in the case of a hyper-production or hypo-production of extracellular matrix or matrix degrading enzymes by tumour cells. This incorrect balance is, for instance, characteristic of fibrosis. Finally, Section 5 considers the spatially-dependent situation showing how the phenomena described from an analytical point of view in Section 4 manifest themselves in a spatial domain where however the overcompression of hyperplasia with respect to the healthy tissue causes the progressive invasion of the tissue. A qualitative description of the travelling wave solution is also given. The velocity of invasion grows with the level of incorrect sensing of stress, in particular it is proportional to the square root of the difference of the volume ratio at which abnormal and normal cells stop duplicating.

2 Phenomenological Description

It is well known that the rate of proliferation of most cells decreases when they come in contact. This phenomenon is often called contact inhibition of growth [42, 44, 65, 81, 88, 99]. A quantification of this phenomenon is represented in Fig. 1 that reports some experimental results by Tsukatani et al. [107] on human breast epithelial cells grown in vitro over a suitable substratum. It can be seen that after an initial exponential growth cell density saturates.

Several experimental papers describe how the starters of the phenomenon are the cadherins, the transmembrane receptors involved in homophilic cell-cell interactions, because of their crucial role in cell-cell adhesion and in mechanotrasduction. It seems that the link between overexpression of cadherins and growth inhibition is a characteristic shared by all types of cadherins. For instance, there are results regarding N-cadherins in Chinese Hampster Ovary [73], in vascular smooth muscle cells [110], and in epithelial cells of the inner ear [112], E-cadherins in human breast epithelial cells [99, 107], and in epithelial and fibroblastoid cells [101], VE-cadherins in vascular endothelial cells [27, 81], T-cadherins in neuronal cells [105].

The direct involvement of cadherins was checked in several ways. For instance, Warchol [112] found that the interaction of cells with synthetic beads coated with N-cadherin ligands spread over the substratum on which the cells live leads to growth arrest at the G1 phase of the cell-cycle. Similarly, Caveda et al. [27] found that coating the underlying substratum with the extracellular domain of recombinant VE-cadherin suppresses cell proliferation.

In addition to confirming that the expression of exogenous E-cadherin arrests cell growth Stockinger et al. [101] also found that a prolonged expression of E-cadherin may cause apoptosis.
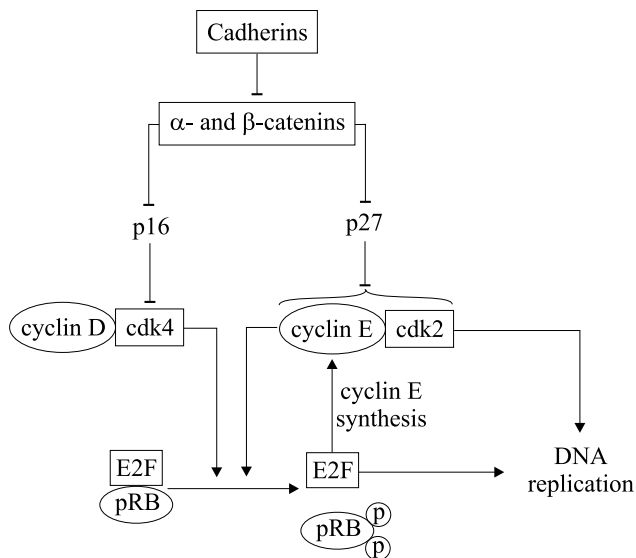
Figure 2: Sketch of the protein cascade involved in contact inhibition of growth. cdk stands for cyclin-dependent kinase, pRB for hypophosphorilated retinoblastoma, and the added p's indicate its phosphorilation. Partly modified from [44]. The usual arrow indicates a stimulatory action, while the other arrow indicates an inhibitory action. The curly bracket indicates that p27 binds to the cdk2/cyclin complex.

Conversely, Castilla et al. [25] found that the disruption of the intercellular cadherin junctions triggers the production of growth factors which contribute to induce proliferation.

By this mechanism the loss of contact responsiveness can lead to deregulated growth, a phenomenon which is commonly associated with the formation of hyperplasia and malignant transformation such as gastric carcinoma [11, 83], adenocarcinoma [108], epithelial tumours [26, 36], colon polyps and carcinoma [52], gynecological cancers [95], intimal thickening [109] (see also the review by Hajra and Fearon [56]). Actually, Cavallaro et al. [26] considered this misperception of the presence of neighbouring cells as a fundamental milestone in the development of tumours naming it "cadherin switch" in analogy with the "angiogenic switch" leading to the vascularization of tumours.

However, cadherins represent the visible side of the process because of their transmembrane location. In fact, there are many other actors on the backstage that can be involved in the incorrect mechano-transduction, first of all catenins, the proteins cadherin link to for a functional cell adhesion. The cadherin-catenin relation is well described by George and Dwivedi [51]. For instance, Stockinger et al. [101] found that when epithelial cells are grown in vitro at low densities ($\leq 40\%$ confluency), they exhibited an increased β-catenin activity, which was five- to sevenfold reduced when cells reached a confluency $> 80\%$. Then in physiological conditions upon reaching confluency the expressed cadherins sequester catenins downregulating their activity, so that as a final result cell adhesion negatively affects cell proliferation.

Conversely, upregulation of catenins is known to induce cell proliferation by a cascade of events which will be explained in the following and is sketched in Fig. 2. In order to test the association with catenins Caveda et al. [33] transfected Chinese Hampster Ovary cells with a cytoplasmic truncated mutant of VE-cadherin. They found that the deletion of the cytoplasmic tail does not affect the adhesive properties of VE-cadherin. However, it abolishes its growth inhibitory activity.

In more detail, as explained in Dietrick et al. [44], the mechanism of contact inhibition of growth seems to be the following: the underexpression of catenins, which can be due to cell contact and overexpression of cadherins, determines the accumulation of the cyclin-dependent kinase (cdk) inhibitors p16, p21, and p27. Their overexpression inhibits the entry in the S phase causing cell cycle arrest in the G1 phase [38, 65, 88]. The increase of cellular levels of the cdk inhibitor p27 was for instance observed in epithelial cells growing to confluence by

4

Polyak et al. [88] and in fibroblasts by Hengst et al. [58] and Winston et al. [113]. The accumulation is partly due to a translational upregulation, partly due to increased half-life of p27 in response to decreased degradation by the ubiquitin-proteasome pathway [59]. In more detail, referring to Fig. 2, p16 blocks the activity of cdk4 by dissociating cyclin D from cdk4 and binding to cdk4. On the other hand, p27 inhibits cdk2-cyclin E directly by binding to the complex (see also [89] who also study the influence of transforming growth factor-β in the process).

Conversely, still referring to Fig. 2, upregulation of catenins leads to the expression of cyclin dependent kinase and then to DNA replication and mitosis.

As a further confirmation of the above cascade of events Dietrick et al. [44] found that in contact inhibited cells the relative levels of hypophosphorilated retinoblastoma (pRB) increase.

It seems that catenin is an important crossing of several cascades leading to contact inhibition of growth. For instance, it has been recently found that α and β-catenins bind to the tumour suppressor gene product adenomatous polyposis coli (APC) and APC mutations in the region responsible for binding to catenins are associated with the developement of hyperplasia, which, as already mentioned, is an early event in tumorigenesis [97, 102].

Barker and Clevers [10] describe how the growth suppressive-effect of E-cadherin requires the presence of its cytoplasmic β-catenin interaction domain, how catenin overexpression is related to Wnt signalling, and how catenin transcriptional activity is implicated in inducing hyper-proliferation in various tumours. In fact, it was found that increased β-catenin transcriptional activity upon overexpression of stable activated β-catenin in the intestine [55] or of truncated β-catenin in the skin [49] of transgenic mice leads to the development of intestinal polyp and hair tumours, respectively. β-catenin mutations have been detected in many other tumours, suggesting that a decreased cadherin/catenin association contributes to neoplastic formation [56]. In this paper, without being specific, we work under the assumption that something goes wrong in the cascade of events mentioned above generating an imperfect mechano-transduction relative to the compressed state of a cell and therefore an abnormal duplication of cells.

Another issue to keep in mind in developing a macroscopic model of growing tissues is that they are not in a stress-free configuration (see [37, 47, 98, 104]). Actually, it seems that cells prefer to feel a moderate amount of stress (see [96] and references therein). A residual stress is in fact present in many cases and may be related to differential growth [3, 6, 61]. For this reason in the model to follow we will include the possibility of duplication at moderate levels of compression.

The other main component considered in this paper is the extracellular matrix (ECM) which is composed by many constituents produced by a variety of stromal cells, mainly fibroblasts. In this paper we do not distinguish among the different types of cells in the tissue, but only distinguish between normal and abnormal cell populations and stroma. In this sense, we will generally say that the cell population produces ECM.

The percentage of cells and ECM changes considerably from tissue to tissue. For instance, the skeletal muscle collagen volume fraction is 14%, that for corneal stroma is 29% and that for subcutaneous tissue is 21% [74]. Tendons consists of 55-70% of water and a substantial part of this is associated with proteoglycans in the ECM. Of the tendon dry weight, 66-85% is collagen [67].

Regarding the rate of production, in vitro endogenous proteins such as fibronectin and von Willebrand factor are released by endothelial cells so that a complex matrix is organised within a few hours after seeding [33, 41].

The ECM is then continuously renewed and remodelled through both the production of matrix metallo-proteinases (MMP) and the synthesis of new ECM components. In stationary physiological conditions the remodelling of ECM is much slower than when a new tissue has to be produced. For instance, in the human lung the physiological turnover of total ECM is 10-15% per day [63], which means that a complete turnover occurs in nearly a week. Our understanding is that upon reaching confluency the cells slow down the production of ECM components.

It is however well known that the remodelling process is strongly affected by the stresses and strains the tissue is subject to. This is classically known for bones and teeth [77] and muscles [66, 67] and is physiologically functional because it allows to keep the stroma young and reactive. In fact, prolonged rest or space flight are detrimental for bones and muscles, while exercise and physical training have an opposite effect. It is common knowledge that traction is applied to heal fractures or to govern the growth of mandibular bones in children. More specifically, in bones mechanical strain induces MMP-13 expression through MEK-ERK signalling pathway [115].

Experiments to quantify the production of ECM mainly under cyclic stretch conditions have been performed

by several authors (see, for instance, [16, 34, 39, 66, 72, 115]). Increased production of ECM, growth factor production and collagenase activity was also generated by mechanically stimulating cardiac fibroblasts [76].

Several authors studied the differences between the chemical and morphological characteristics of the ECM of normal tissues and that of tumours. For instance, Takeuchi et al. [106] found that breast tumours presented a denser and more fibrous stroma, with variation in the content of hyaluronic acid, glycosaminoglycans, condroitin sulfate and dermatan sulfate among other components (see also [2, 78, 111]). Variations in the contents of type I collagen [70], fibronectin and laminin [21, 35] were also observed. Christensen [35] also argued that the variations above can be due to increased production by the tumour cells.

Increased expression of fibronectin not balanced by increased collagenase activity was also observed in other occasions like cardiac hyperthrophy, cardiac fibrosis, liver fibrosis, pulmonary fibrosis, asthma, glomerulonephritis, colon cancer [20, 63, 76, 92]. In intima hyperplasia, both the amount of cells and of ECM increase [82]. Johnson [63] argued that the alteration in the ECM components can be due to several probably concurring reasons: increased de novo synthesis of ECM proteins, decreased activity of its degrading enzyme (MMP), and upregulation of the tissue-specific inhibitors of metalloproteinases (TIMP).

On the other hand, excessive degradation of ECM due to excessive production of MMP-13 characterizes chronic inflammatory diseases such as osteoarthritic cartilage, rheumatoid synovium, chronic ulcer, intestinal ulcerations, periodontitis, and many malignant tumours [115].

The composition of ECM also changes with tumour progression and is so important in determining cell growth, differentiation and movement that Liotta and Kohn [75] mention the possibility of finding a "stromal therapy as a new strategy" against cancer. Referring to the changes of ECM content with tumour progression, for instance, Zhang et al. [116] showed that the content of collagen fibers increased with prostate cancer grade ranging from nearly 7% to 26% of the area analysed.

3   The Mathematical Model

In constructing the model we refer to the volume ratio related to both normal and abnormal cells and extracellular matrix, i.e. the fraction of volume occupied by the single constituents. We will use the term "abnormal cells" to denote in general those cells which respond in a physiologically different way to compression and might give rise to a tumour at some later stage in their evolution. Abnormal extracellular matrix will be that produced by such abnormal cells.

To be more precise

- n is the volume ratio occupied by normal cells;

- a is the volume ratio occupied by tumour cells;

- m_n is the volume ratio occupied by host extracellular matrix (ECM).

- m_a is the volume ratio occupied by extracellular matrix produced by tumour cells, which is known to be structurally and chemically different from that produced by normal cells [2, 70, 78, 106, 111].

These state variables are then already dimensionless and are in the range $[0, 1]$. Considering that, as explained in the previous section, their values strongly depend on the tissue considered, throughout the paper we will work with a virtual tissue made of 50% of cells, 20% of ECM and 30% of extracellular liquid, which means that $n \approx 0.5$ and $m_n \approx 0.2$.

In addition to the volume ratios above, another fundamental state variable is

- c, the concentration of matrix degrading enzymes (MDEs), e.g. the plasminogen activators or matrix metalloproteinases.

On the contrary of cells and ECM, MDEs are considered as macromolecules which diffuse in the extracellular liquid without occupying space.

In the following an important role will be played by the overall volume ratio occupied by cells and extracellular matrix

$$\psi = n + a + m_n + m_a. \tag{1}$$

and by its relation with the stress. In using (1) it is assumed for simplicity that all cells and matrix constituents of any origin contribute equally to the sensing of stress by the cells. A discussion of this hypothesis is given in [40] where alternatives are also proposed.

Several forms of stress-volume ratio relations can be taken into account [7, 23]. The simplest features characterizing stress are that it vanishes below a value ψ_0, which we denote stress-free volume ratio and corresponds to the confluent volume ratio, is increasing for $\psi > \psi_0$ and tends to infinity at $\psi = 1$, e.g.

$$\Sigma(\psi) = E(1 - \psi_0) \left(\frac{\psi - \psi_0}{1 - \psi} \right)_+ , \tag{2}$$

where f_+ is the positive part of f and E is the value of the derivative in $\psi = \psi_0$, a sort of Young modulus for moderate compressions. However, since usually $\psi \approx \psi_0$, then one can also approximate Eq.(2) with $\Sigma(\psi) = E(\psi - \psi_0)_+$. We explicitly mention that the constitutive relation (2) is not able to describe the response to tensile stresses and adhesion-like behaviours.

The mass balance equations for the two types of cells in our model then write as

$$\frac{\partial n}{\partial t} + \nabla \cdot (n\mathbf{v}_n) = \Gamma_n n - \delta_n n \,,$$

$$\frac{\partial a}{\partial t} + \nabla \cdot (a\mathbf{v}_a) = \Gamma_a a - \delta_a a \,. \tag{3}$$

where we will consider the death coefficient to be constant, though apoptosis may be influenced by the stress level [57].

Referring to the phenomenological discussion presented in the previous section, we assume that cells replicate if they feel there is sufficient space to do this, that is if they can sense a sustainable level of compression ($\psi \leqslant \psi_n$), or equivalently stress ($\Sigma \leqslant \Sigma_n$ with $\Sigma_n = \Sigma(\psi_n)$). Our assumption is that the threshold value ψ_n is nearly equal to the stress-free value ψ_0 for normal cells and slightly larger for abnormal ones ($\psi_a > \psi_n$). Actually, growth might even be independent of ψ (or equivalently $\psi_a \geq 1$), meaning that the cells are completely insensitive to mechanical cues and continue replicating independently of the compression level.

To describe what stated above, we choose the simplest possible switch mechanism depending on compression for the growth coefficient

$$\Gamma_n(\psi) = \gamma_n H_\sigma(\psi - \psi_n) \,,$$

$$\Gamma_a(\psi) = \gamma_a H_\sigma(\psi - \psi_a) \,, \tag{4}$$

where H_σ is a monotonic mollifier of the step function with the properties that it is a continuous function with $H_\sigma(\phi) = 1$ if $\phi \leqslant 0$ and $H_\sigma(\phi) = 0$ if $\phi \geqslant \sigma$. In particular, we will choose

$$H_\sigma(\phi) = \begin{cases} 1 & \text{if} \quad \phi \leq 0; \\ 0 & \text{if} \quad \phi > \sigma; \\ 1 - \frac{\phi}{\sigma} & \text{otherwise}; \end{cases} \tag{5}$$

We explicitly notice that for $\psi_n > \psi_0$, H_σ can be equivalently defined as a switch mechanism based on the stress level. In fact, in the following we will often make use of the correspondence between compression and stress.

Of course, the growth term depends on other quantities, e.g. the amount of nutrient and growth factors. In this paper, however, we want to focus on the possible role of compression and stress on tumour invasion and therefore assume that all nutrients are abundantly supplied and neglect the effect of growth factors. In doing this we tacitly assume that all the constituents necessary for the cell to grow and undergo mitosis can be found in the extracellular liquid that is a passive constituent in the global mass balance equation. Actually, in the following examples we will consider the case in which $\gamma_n = \gamma_a$ meaning that the reproduction rate is the same and only the stress perception is different $\psi_n < \psi_a$. For the same reason we will not consider other mechanisms such as the reduced viability of normal tissue in a low pH-environment [50].

Regarding the motion of normal cells, observing that they move in the intricate network formed by the extracellular matrix (see the supplementar material for [114]), we model the ensemble of cells as a granular material in a porous medium. Therefore, following [7, 91], we can write the momentum equation for the cells

$$\rho n \left(\frac{\partial \mathbf{v}_n}{\partial t} + \mathbf{v}_n \cdot \nabla \mathbf{v}_n \right) = \nabla \cdot \mathbf{T}_n + \mathbf{m}_n \,, \tag{6}$$

which neglecting inertia and introducing the usual porous media assumptions on the stress tensor $\mathbf{T}_n$ and on the interaction force $\mathbf{m}_n$ leads to

$$\mathbf{v}_n = -K\nabla\Sigma(\psi) \,, \tag{7}$$

where K is related to the permeability of the medium.

In addition, we explicitly mention that in many of the cases that we will deal with in the following sections, the exact form of the stress-volume ratio relation is of minor importance.

The coefficient K is not only related to the pure permeability of the porous medium but also to the ability of cells to move through the ECM network. It will in fact depend on the amount of ECM for two main reasons: space occupation and presence of adhesion sites. Actually, increased motility is observed for regions with higher concentration of ECM. However, it decreases again for large values of ECM concentration because of the increase of adhesive sites (see [60, 85, 87]).

The closure (7), phenomenologically introduced in [15, 53], has the effect to push cells away from the overcrowded region where they feel pressed, until they reach, if possible, a stress-free configuration. In mathematical terms this means that the motion is down the stress gradient, or the overall density gradient.

In the following we will assume that normal and abnormal cells behave in the same way under compression, i.e.

$$\mathbf{v} \equiv \mathbf{v}_a = \mathbf{v}_n = -K\Sigma'(\psi)\nabla\psi \,, \tag{8}$$

so that Eq.(3) rewrites as

$$\frac{\partial n}{\partial t} = \nabla \cdot [nK\Sigma'(\psi)\nabla\psi] + [\gamma_n H_\sigma(\psi - \psi_n) - \delta_n]n \,,$$

$$\frac{\partial a}{\partial t} = \nabla \cdot [aK\Sigma'(\psi)\nabla\psi] + [\gamma_a H_\sigma(\psi - \psi_a) - \delta_a]a \,. \tag{9}$$

Coming to the extracellular matrix, as has already been mentioned, this is a intricate network of fibrous material made of many macromolecules, including fibronectin, laminin and collagen, which can be degraded by MDEs [28, 79, 86, 100]. Active MDEs are produced (or activated) by the cells, diffuse throughout the tissue and undergo some form of decay, either passive or active. The equation governing the evolution of MDE concentration is therefore given by

$$\frac{\partial c}{\partial t} = \kappa\nabla^2 c + P(n, a, c, \Sigma) - D(c, m)c \,. \tag{10}$$

The functions P and D model the production of active MDEs by normal and abnormal cells and their decay, respectively. We will take $D = 1/\tau$ to be a constant (other functional forms for D have also been investigated, see [8] for details) and P to be of the following form

$$P = \pi_n(\Sigma)n + \pi_a(\Sigma)a \,. \tag{11}$$

In the following we will consider in more detail the case in which π_n and π_a are constant.

Upon contact, MDEs degrade the extracellular matrix produced by the cells in a stress-dependent way. Hence the degradation process can be modelled by the following simple equations

$$\frac{\partial m_n}{\partial t} = \mu_n(\Sigma)n - \nu c m_n \,,$$

$$\frac{\partial m_a}{\partial t} = \mu_a(\Sigma)a - \nu c m_a \,, \tag{12}$$

where ν is a positive constant and μ_n and μ_a depend on whether the cells are in a confluent situation or not, or on the fact that the tissue is subject to strain. In most of the simulations to follow we will take them as constant. The study of the case in which π_i and μ_i $(i = n, a)$ depend on the level of stress, which as already mentioned is of great interest in tissue remodelling, is left as a future development when more quantitative experimental data on these dependences are available.

In (12) we distinguish the production of ECM by normal and abnormal cells, because as explained in the previous section, they are morphologically and chemically different. In addition, the production rates can be different, while it is known that the degradation by MDEs does not distinguish between the two types of ECM.

Summarizing, the complete system of equations is

$$
\begin{cases}
\dfrac{\partial n}{\partial t} = \overbrace{\nabla \cdot [nK\Sigma'(\psi)\nabla\psi]}^{\text{response to compression}} + \overbrace{\gamma_n H_\sigma(\psi - \psi_n)n}^{\text{growth}} - \overbrace{\delta_n n}^{\text{apoptosis}}\,, \\[2ex]
\dfrac{\partial a}{\partial t} = \overbrace{\nabla \cdot [aK\Sigma'(\psi)\nabla\psi]}^{\text{response to compression}} + \overbrace{\gamma_a H_\sigma(\psi - \psi_a)a}^{\text{growth}} - \overbrace{\delta_a a}^{\text{apoptosis}}\,, \\[2ex]
\dfrac{\partial m_n}{\partial t} = \overbrace{\mu_n(\Sigma(\psi))n}^{\text{host production}} - \overbrace{\nu c m_n}^{\text{degradation}}\,, \\[2ex]
\dfrac{\partial m_a}{\partial t} = \overbrace{\mu_a(\Sigma(\psi))a}^{\text{tumour production}} - \overbrace{\nu c m_a}^{\text{degradation}}\,, \\[2ex]
\dfrac{\partial c}{\partial t} = \overbrace{\kappa\nabla^2 c}^{\text{diffusion}} + \overbrace{\pi_n(\Sigma(\psi))n}^{\text{host production}} + \overbrace{\pi_a(\Sigma(\psi))a}^{\text{tumour production}} - \overbrace{\dfrac{c}{\tau}}^{\text{decay}}\,.
\end{cases}
\tag{13}
$$

where H_σ and Σ are defined by (2) and (5), respectively and we recall that $\psi = n + a + m_n + m_a$ is the percentage of volume not occupied by the extracellular liquid.

4 Qualitative Behaviour of Spatially Independent Solutions

Before proceeding with the numerical simulation of the full model, we consider some simple cases in order to understand and describe the main features of the model presented above working in the spatially homogeneous case. This allow to give the analytical form of some significant spatially independent solutions.

4.1 Generation of Confluent Distribution in Vitro

In order to compare the results of the models with some experiments in vitro as the one shown in Fig. 1 and to identify some of the parameters of the model, we start with the easiest situation in which a few cells are uniformly seeded on a suitable substratum in a Petri dish and, duplicating on the surface of the substratum, grow to confluence with no production of extracellular matrix. This situation is modelled by

$$
\frac{\partial n}{\partial t} = [\gamma_n H_\sigma(n - \psi_n) - \delta_n]n\,,
\tag{14}
$$

which for H_σ given by (5) can be easily solved by

$$
n = \begin{cases}
n_0 \exp[(\gamma_n - \delta_n)t] \qquad \text{for} \quad t \le t_0; \\[3ex]
\dfrac{\psi_n + \left(1 - \dfrac{\delta_n}{\gamma_n}\right)\sigma}{1 + \left(1 - \dfrac{\delta_n}{\gamma_n}\right)\dfrac{\sigma}{\psi_n}\exp\left[-\left(\gamma_n - \delta_n + \gamma_n\dfrac{\psi_n}{\sigma}\right)(t - t_0)\right]} \qquad \text{for} \quad t > t_0;
\end{cases}
\tag{15}
$$

9

Cell type	Duplication time (hours)	Growth rate (days^{-1})	Source
CHO	18–19	0.86–0.91	[73]
CHO	14–21	0.8–1.2	[27]
L929	10–12	1.4-1.6	[27]
Fibroblast	16.2	1.03	[101]
HBE	22.3	0.746	[107]
BPAEC	38–44	0.38–0.44	[81]

Table 1: Growth rates for different cell types. CHO stands for Chinese Hampster Ovary cells, HBE for Human Breast Epithelial cells BPAEC for Bovin Pulmonary Artery Endothelial Cells.

where $n_0 < \psi_n$ is the initial volume ratio of cells and

$$t_0 = \frac{1}{\gamma_n - \delta_n} \ln \frac{\psi_n}{\sigma} \tag{16}$$

is when confluency starts. The solution will tend toward the volume ratio

$$n_\infty = \hat{\psi}_n := \psi_n + \left(1 - \frac{\delta_n}{\gamma_n}\right)\sigma, \tag{17}$$

which, even if $\psi_n = \psi_0$, implies a small compression of the tissue $\Sigma \approx E(1 - \frac{\delta_n}{\gamma_n})\sigma$. In Fig. 1 we compare the results of the experiments by Tsukatani et al. [107] and Eq.(15) for the doubling time $T = 22.3$ h ($\gamma_n = 0.746$ days^{-1}) measured therein and for different values of σ assuming that the stationary cell density measured there ($N = 69000$ cells over a 35 mm dish) correspond to $\psi_n + \sigma = 0.7$. In the experiments by Tsukatani et al. [107] an unexplained decrease of cell population in the first day is measured. For this reason the cell density measured 48 hours after seeding was taken as initial condition for Eq. (14) ($N_0 = 45000$ cells over a 35 mm dish, corresponding to $n_0 = 0.495$). From the simulation it appears that $\sigma \approx 0.2$. For sake of completeness in Table 1 we report the growth rates measured for different cell types.

4.2   Generation of Normal Tissue

We consider now how the model describes the re-construction of a normal tissue starting from few cells $n_0 < \psi_n$ constantly distributed in space. Possibly, in the same region there might be a small constant amount of extracellular matrix, so that at least initially $n + m_n < \psi_n$. In this case the system initially reduces to

$$\begin{cases} \dfrac{\partial n}{\partial t} = [\gamma_n H_\sigma(n + m_n - \psi_n) - \delta_n]n\,, \\[2mm] \dfrac{\partial m_n}{\partial t} = \mu_n n - \nu c m_n\,, \\[2mm] \dfrac{\partial c}{\partial t} = \pi_n n - \dfrac{c}{\tau}\,, \end{cases} \tag{18}$$

Denoting by $\hat{\psi}_n \in [\psi_n, \psi_n + \sigma]$ the value such that $H_\sigma(\hat{\psi}_n - \psi_n) = \delta_n/\gamma_n$ (given by (17) if H_σ is given by (5)), the steady state can easily be written down.

$$n = \hat{\psi}_n - M_n\,, \qquad m_n = M_n\,, \qquad c = \pi_n \tau (\hat{\psi}_n - M_n)\,, \tag{19}$$

where

$$M_n = \frac{\mu_n}{\nu \pi_n \tau}\,. \tag{20}$$

10

In particular, the ratio of cells to ECM is

$$\eta := \frac{n}{m_n} = \frac{\nu \pi_n \tau}{\mu_n} \hat{\psi}_n - 1 \,, \tag{21}$$

which is an easily measurable value (approximately $\eta = 2$). We observe that M_n has to be smaller than 1, otherwise the production of ECM would never be balanced by degradation leading to the formation of a tissue only made of ECM with no cells.

In order to explicit the analytical form of the solution, the discussion proposed in this and in the following subsections holds in the limit $\sigma \to 0$. In fact, for instance, in this case Eq.(18) can be solved in cascade. However, for sake of simplicity, considering that MDE production and degradation is much faster than cell duplication we only write here the solution obtained under the assumption that $c(t) \approx \pi_n \tau n(t)$. In this case the solution writes as

$$n = n_0 \exp[(\gamma_n - \delta_n)t] \,, \tag{22}$$

$$m_n = M_n + (m_0 - M_n) \exp\left[\frac{\nu \pi_n \tau n_0}{\gamma_n - \delta_n}\left(1 - e^{(\gamma_n - \delta_n)t}\right)\right] \,, \tag{23}$$

till $m_n(t) + n(t)$ reaches ψ_n. From this instant, which will be denoted by $\hat{t}$ and can be determined through an implicit relation, $n(t) = \psi_n - m_n(t)$ where $m_n(t)$ satisfies

$$\frac{\partial m_n}{\partial t} = \mu_n \left(1 - \frac{m_n}{M_n}\right)(\psi_n - m_n) \,, \tag{24}$$

which is solved by

$$m_n = \frac{M_n + \psi_n \frac{\hat{m}_n - M_n}{\psi_n - \hat{m}_n} \exp\left[-\mu_n \left(\frac{\psi_n}{M_n} - 1\right)(t - \hat{t})\right]}{1 + \frac{\hat{m}_n - M_n}{\psi_n - \hat{m}_n} \exp\left[-\mu_n \left(\frac{\psi_n}{M_n} - 1\right)(t - \hat{t})\right]} \,, \tag{25}$$

where $\hat{m}_n = \psi_n - n_0 \exp[(\gamma_n - \delta_n)\hat{t}]$ is the ECM volume ratio reached at $t = \hat{t}$.

(Ricontrolla tutto questo)

Before proceeding with the simulation let us quantify, as far as possible, the parameters involved. From the observation that in vitro cells organise an ECM within a few hours after seeding [33, 41] we infer that $\mu_n \approx 10$ days^{-1}. On the other hand, from the fact that 10-15% of the lung ECM is renewed every day [63] we can evaluate $\mu_n \approx 0.1$ days^{-1}. This suggests that the ECM production decreases while cells achieve a confluent configuration. In most of the following simulations we will use a value near the lower bound because we usually deal with ECM remodelling.

The other parameters directly measured are the diffusion coefficient of MDEs $\kappa = 0.85 \times 10^{-6}$cm^2/sec [14] and the MDEs half life which of course depend on the specific enzyme and may span in the range $10^{-4} - 0.13$ h [62, 84]. This means that the range of action $\xi = \sqrt{\kappa \tau}$ of the various MDEs span from few microns, i.e. a very local action, to few hundred of microns, which is one order of magnitude less than the typical size of an avascular tumour in its steady state. However, to consider the entire chain of reactions we will take a value near the upper limit for τ.

Since it seems that the usual concentration of MDEs is about 15000 molecules/μm^2 [64] and the steady value foreseen by the model is $c_\infty = \pi_n \tau n_\infty$, then we assume that $\pi_n \approx 10^6 - 10^7$ molecules/μm^2 days. Since we are working with an ideal tissue made of 20% ECM, then $\nu \approx \times 10^{-5}$ μm^2/molecules days.

Finally, the apoptotic rate δ_n which has to be less than γ_n is assumed to be 0.1 days^{-1}.

The corresponding values for abnormal tissue are slight modification of the values above.

The estimates above have been used in the simulation given in Fig. 3. The solution presents an overshooting because of the fact that the volume ratios of ECM and cells do not reach the stationary value at the same time. In fact, production rates are different. In particular, in Fig. 3a the production of ECM is quite slow, because right from the beginning the ECM production rate is of the order of the value estimated at the steady state. Instead, in Fig. 3b $\mu_n = 10(1 - \psi)^4$ days^{-1} is chosen as an example of decreasing production of ECM. The difference with Fig. 3a consists in a larger production of ECM at earlier times which determines an initial overproduction of ECM occupying up to twice the volume in the final configuration. The extra ECM is then progressively degraded by the MDEs to reach the stationary value $\mu(\hat{\psi}_n)/\nu \pi_n \tau$.
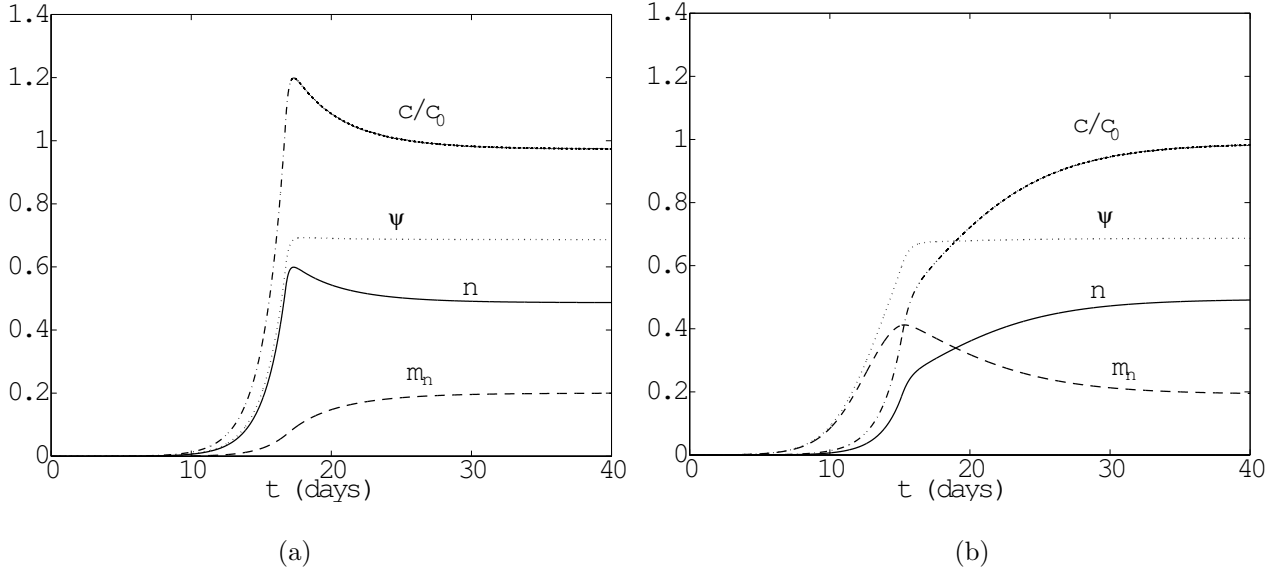
Figure 3: Generation of a normal tissue in the case of a constant slow production of ECM (a) and of a density dependent production approximating a fast production at early times and a slow stationary production at confluency (b). The values of the parameters are $\gamma_n = 0.746$ days^{-1}, $\delta_n = 0.1$ days^{-1}, $\pi_n/c_0 = 400$ days^{-1}, $\nu c_0 = 0.25$ days^{-1}, $\tau = 0.005$ days, $\psi_n = 0.6$, $\sigma = 0.1$ where c_0 is the reference concentration value 15000 molecules/μm^2. In (a) $\mu_n = 0.1$ days^{-1}. From bottom to top, volume ratio of ECM, cells and overall volume ratio and normalized MDE concentration. In (b) $\mu_n = 10(1-\psi)^4$ days^{-1} leading to a faster initial production of ECM and a temporary hyperproduction of ECM.

Parameter	Estimated value	Source
δ	0.1 days^{-1}	see text
μ_n	$0.1 - 10$ days^{-1}	[33, 41, 63]
ν	$10^{-5} \frac{\mu\text{m}^2}{\text{molecules days}}$	see text
π_n	$10^6 - 10^7 \frac{\text{molecules}}{\mu\text{m}^2 \text{ days}}$	see text
τ	$\frac{1}{6}$ sec - 0.13 h	[62, 84]
κ	$0.85 \times 10^{-6} \frac{\text{cm}^2}{\text{sec}}$	[14]

Table 2: Parameter estimate.

4.3 Development of Abnormal Tissue

Assume now that by a clonal differentiation some abnormal cells appear in the fully developed tissue. We first assume that they appear constantly throughout the domain, so that we can take for the system

$$\begin{cases} \dfrac{\partial n}{\partial t} = [\gamma_n H_\sigma(\psi - \psi_n) - \delta_n]n\,, \\[2ex] \dfrac{\partial a}{\partial t} = [\gamma_a H_\sigma(\psi - \psi_a) - \delta_a]a\,, \\[2ex] \dfrac{\partial m_n}{\partial t} = \mu_n n - \nu c m_n\,, \\[2ex] \dfrac{\partial m_a}{\partial t} = \mu_a a - \nu c m_a\,, \\[2ex] \dfrac{\partial c}{\partial t} = \pi_n n + \pi_a a - \dfrac{c}{\tau}\,, \end{cases} \tag{26}$$

a natural modification of the stationary solution (19)

$$n(t = 0, x) = \psi_n - a_0 - M_n\,,$$

$$a(t = 0, x) = a_0\,,$$

$$m_n(t = 0, x) = M_n\,, \tag{27}$$

$$m_a(t = 0, x) = 0\,,$$

$$c(t = 0, x) = \pi_n \tau (\psi_n - M_n)\,,$$

as initial conditions where M_n is defined in (20).

We start by assuming that the rates of productions of ECM and MDEs are equal ($\mu_n = \mu_a$ and $\pi_n = \pi_a$). The equations for the ECM can then be added to give

$$\frac{\partial m}{\partial t} = \mu_n(n + a) - \nu c m\,, \tag{28}$$

where $m = m_n + m_a$.

Observing, as in the previous subsection, that the timescales of production and degradation of MDEs are much faster than the time of reproduction of the cells and of production of the more complex ECM (minutes with respect to hours or days, see Table 2), we can state that the concentration of MDEs quickly reaches the value

$$c = \pi_n \tau (n + a)\,, \tag{29}$$

which can be substituted back in (28) to obtain

$$\frac{\partial m}{\partial t} = \mu_n \left(1 - \frac{\pi_n \nu \tau}{\mu_n} m\right)(n + a)\,. \tag{30}$$

Therefore, from the initial conditions, one has that

$$m(t) = m_n(t) + m_a(t) = M_n\,,$$

remains constant which, in particular, implies $\psi(t) = n(t) + a(t) + M_n$ at all times.

We can then focus on the first two equations to explain first how the abnormal cells progressively replaces the normal ones in the tissue.

13

Since $\psi_n < \psi_a$, initially the abnormal tissue continues its proliferation and

$$a(t) = a_0 e^{(\gamma_a - \delta_a)t} . \tag{31}$$

A similar solution would hold for the normal tissue if $\psi \leqslant \psi_n$, but this contradicts the fact that all populations grow starting from an initial condition with $\psi = \psi_n$. Hence throughout the process $\psi \geqslant \psi_n$.

On the other hand, whenever $\psi > \psi_n$ normal cells would decay exponentially. So n cannot overcome the value of the volume ratio corresponding to the natural configuration (actually, when using a mollifier of width σ, the volume ratio $\psi_n + \sigma$).

Similarly to what we have just discussed, initially we cannot have $\psi > \psi_n$ positive, otherwise the total volume ratio would be

$$\psi(t) = (\psi_n - M_n - a_0)e^{-\delta_n t} + a_0 e^{(\gamma_a - \delta_a)t} + M_n , \tag{32}$$

which is smaller than ψ_n for small values of a_0. This simply corresponds to the fact that in an interval of time Δt, an amount $a_0(\gamma_a - \delta_a)\Delta t$ of abnormal cells is produced and a larger amount $(\psi_n - M_n - a_0)\delta_n \Delta t$ of normal cells dies (if $a_0(\psi_n - M_n) < \delta_n/(\gamma_a - \delta_a + \delta_n)$.) What happens is that an amount of normal cells is still produced to adjust ψ to the maximum stress-free value. Therefore,

$$n(t) = \psi_n - M_n - a_0 e^{(\gamma_a - \delta_a)t} , \tag{33}$$

so that $n + a = \psi - M_n$ is constantly equal to ψ_n. This situation continues until the amount of abnormal cells produced equals the amount of normal cells that would normally die. This occurs when the amount A of abnormal cells is such that

$$A(\gamma_a - \delta_a)\Delta t = (\psi_n - M_n - A)\delta_n \Delta t . \tag{34}$$

Hence

$$A = \frac{(\psi_n - M_n)\delta_n}{\gamma_a - \delta_a + \delta_n} , \tag{35}$$

and since $A = a(t_1) = a_0 e^{(\gamma_a - \delta_a)t_1}$, the instant is given by

$$t_1 = \frac{1}{\gamma_a - \delta_a} \log\left(\frac{\delta_n}{\gamma_a - \delta_a + \delta_n} \frac{\psi_n - M_n}{a_0} \right) , \tag{36}$$

and

$$n(t_1) = \frac{\gamma_a - \delta_a}{\gamma_a - \delta_a + \delta_n}(\psi_0 - M_n) . \tag{37}$$

Referring to Fig. 4a, the period $[0, t_1]$ is characterized by a simple partial replacement of normal cells by abnormal cells, keeping the total volume ratio constantly equal to ψ_n (therefore in this phase there is no compression). For this reason we will call this phase *relaxed replacement* or Phase I.

Notice that if the only difference in the behaviour of normal and abnormal cells is in the sensing of stress by the cells, i.e. $\gamma_n = \gamma_a = \gamma$ and $\delta_n = \delta_a = \delta$, then
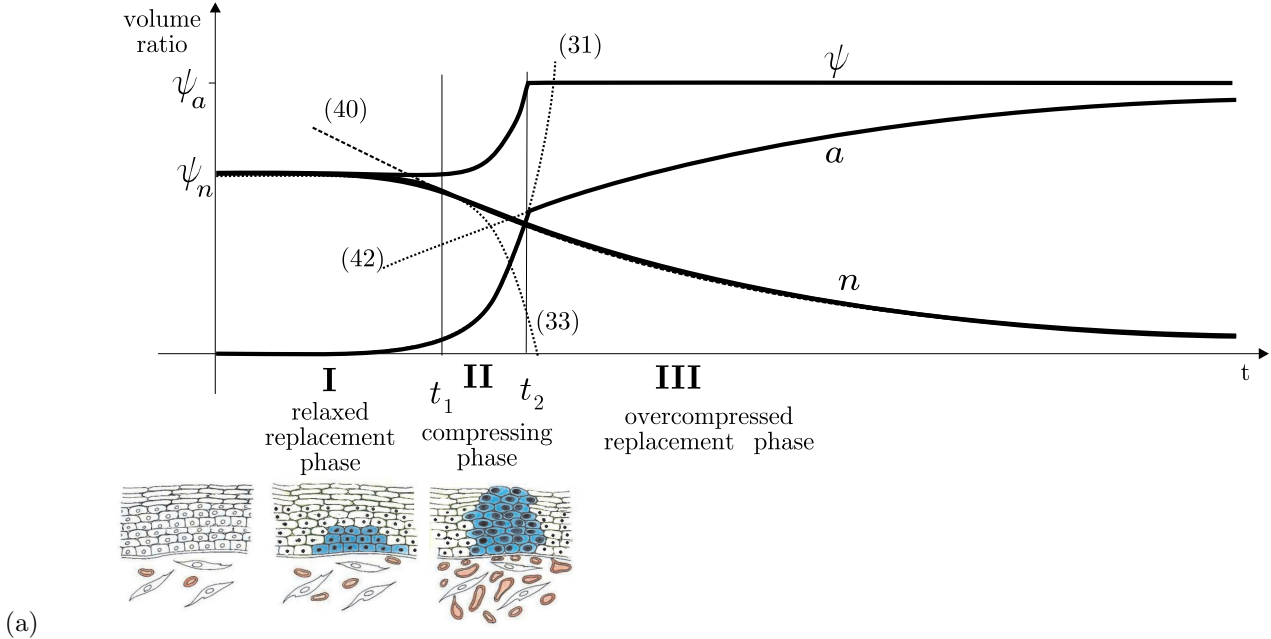
$$t_1 = \frac{1}{\gamma - \delta} \log\left(\frac{\delta}{\gamma} \frac{\psi_n - M_n}{a_0} \right) , \tag{38}$$
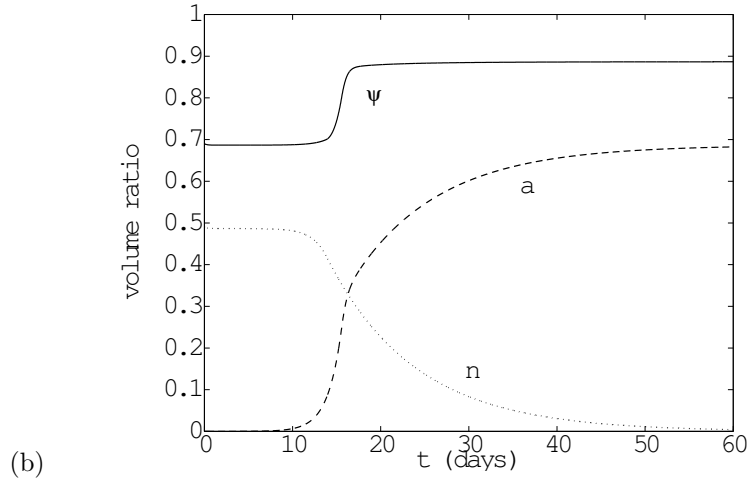
and

$$n(t_1) = \left(1 - \frac{\delta}{\gamma}\right)(\psi_n - M_n), \qquad a(t_1) = \frac{\delta}{\gamma}(\psi_n - M_n) . \tag{39}$$

After the end of the relaxed replacement phase the amount of abnormal cells produced is larger than the amount of normal cells dying, so the total volume ratio starts exceeding the stress-free value ψ_n. Abnormal cells continue to grow satisfying (31) while

$$n(t) = \frac{\gamma_a - \delta_a}{\gamma_a - \delta_a + \delta_n} \left(\frac{\delta_n}{\gamma_a - \delta_a + \delta_n} \frac{\psi_n - M_n}{a_0} \right)^{\frac{\delta_n}{\gamma_a - \delta_a}} (\psi_n - M_n)e^{-\delta_n t} . \tag{40}$$

14

(a)

(b)

Figure 4: Replacement of normal with abnormal cells. In (a) definition of phases of growth and of analytical solutions (dotted lines) in the limit case $\sigma = 0$ (and $m = 0$). The cartoons at the bottom of the Fig. sketch the phenomenological evolution (modified from [54]). In (b) simulation for $\gamma_n = \gamma_a = 1$ days^{-1}, $\delta_n = \delta_a = 0.1$ days^{-1}, $a_0 = 0.00001$, $\psi_n = 0.6$, $\psi_a = 0.8$, and $\sigma = 0.1$. All values of the parameters are equal for the two populations but the stress related thresholds for stopping replication. This implies that the volume ratio of ECM is constantly equal to the initial value $m_0 = 0.2$.
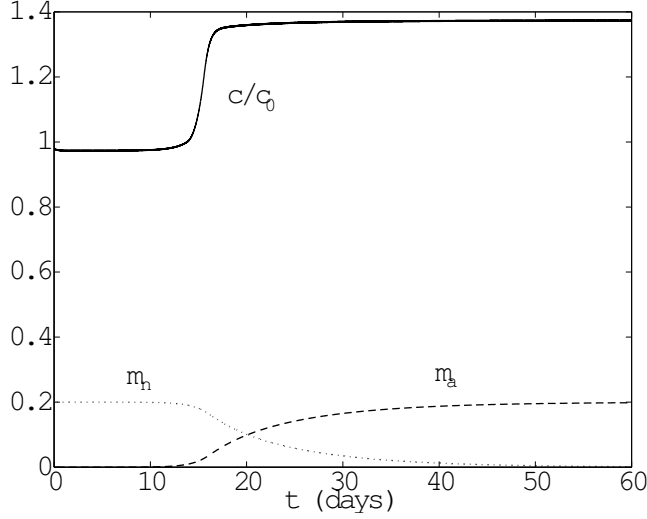
Figure 5: Replacement of ECM in the tissue. Normal ECM (full) is replaced by the one produced by the tumour cells (dashed). Their sum is constantly equal to 0.2. The dotted line describes the evolution of the concentration of MDEs (normalized with respect to the reference value $c_0 = 15000$ molecules/μm^2) that starting from a value controlling the production of normal ECM goes to a value which controls the production of tumour produced ECM. This value is higher because the density of cells is higher (see Fig.4b). The values of the parameters are as in Fig. 4 and $\mu_n = \mu_a = 0.1$ days^{-1} $\pi_n/c_0 = \pi_a/c_0 = 400$ days^{-1}, $\nu c_0 = 0.25$ days^{-1}, $\tau = 0.005$ days.

This change can be identified in Fig. 4 by the change of convexity of the curve related to n. In this second phase

$$\psi(t) = \frac{\gamma_a - \delta_a}{\gamma_a - \delta_a + \delta_n} \left(\frac{\delta_n}{\gamma_a - \delta_a + \delta_n} \frac{\psi_n - M_n}{a_0} \right)^{\frac{\delta_n}{\gamma_a - \delta_a}} (\psi_n - M_n) e^{-\delta_n t} + a_0 e^{(\gamma_a - \delta_a) t} + M_n > \psi_n, \qquad (41)$$

giving rise to a progressive compression of the tissue as in the last cartoon in Fig. 4a. For this reason this phase is called *compressing phase* or Phase II. This situation continues till ψ reaches the value ψ_a.

After this a situation in some sense reciprocal to the relaxed replacement phase occurs, with a decreasing n satisfying (40) while abnormal cells replicate to replace the space left available by n, i.e.,

$$a(t) = \psi_a - n(t), \qquad (42)$$

so that the total volume ratio is constanly equal to ψ_a. This phase then will be called *over-compressed replacement* or Phase III. Eventually, abnormal cells completely replace normal cells.

Focussing now on the two types of ECMs, using (31), (33), (40), and (42) it is possible to solve the related ODEs explicitly. As expected, it is found that m_a increases and m_n correspondingly decreases to zero keeping the sum constant. The concentration of MDEs starting from a value controlling the production of normal ECM goes to a value which controls the production of tumour produced ECM. This value is slightly higher because of the increased density of cells. So, eventually the abnormal stroma completely replaces the normal one, as shown in Figs. 4 and 5.

In conclusion, a very small incorrect sensing of the state of compression by the cells will lead to a clonal advantage and a complete replacement of normal tissue by hyperplasic over-compressed tissue with $a = \psi_a - M_n$, and $m_a = M_n$.

16

4.4 Hyper- and Hypo-Production of ECM and MDEs

If the production of MDEs and/or ECM by the two types of cells occurs at different rates, i.e. $\pi_n \neq \pi_a$ and/or $\mu_n \neq \mu_a$, the steady state mentioned in the previous section modifies to

$$n = m_n = 0\,, \qquad a = \psi_a - M_a\,, \qquad m_a = M_a\,, \qquad c = \pi_a \tau (\psi_a - M_a)\,, \tag{43}$$

where

$$M_a = \frac{\mu_a}{\nu \pi_a \tau}\,, \tag{44}$$

i.e., as in the case of equal production of ECM and MDEs by the two types of cells, the abnormal ECM produced by the abnormal tissue will completely replace the ECM produced by the normal cells. However, in this case the final ECM volume ratio might be different from the initial one and depends on the dimensionless parameter M_a.

In particular, the ratio of the content of ECM produced in the normal and in the abnormal case is

$$\frac{m_n}{m_a} = \frac{\mu_n}{\mu_a} \frac{\pi_a}{\pi_n}\,,$$

coherently with Johnson's observation [63] that the alteration in the ECM components can be due to both increased de novo synthesis of ECM proteins, and decreased activity of its degrading enzyme (MMP), probably together with an upregulation of the tissue-specific inhibitors of metalloproteinases (TIMP).

In Fig. 6 we consider the pathological situation in which the abnormal cells are also characterised by a doubling or halving of the rate of production of ECM (Fig. 6b and 6a, respectively) or of MDEs (Fig. 6c and 6d, respectively).

A hyper-production of ECM (Fig. 6b) and a hypo-production of MDEs (Fig. 6d) lead to a more fibrotic tissue with a ratio of cells versus ECM content nearly equal to 1.22, compared with 2.45 in the physiological situation. On the other hand, a hypo-production of ECM (Fig. 6a) and a hyper-production of MDEs (Fig. 6c) lead to a tissue characterised by a ratio of cells versus ECM content nearly equal to 7.86. In all cases the evolution of ψ and n is very similar to that in Fig. 4b.

If, for instance, both production rates increase keeping the same ratio, then the final configuration would be as in Figs. 4b and 5 and also the evolution of the cell volume ratios would be as in Fig. 4b. However, the ECM turnover would be faster than that shown in Fig. 5.

5 Invasion of Tissue

We now assume that the abnormal tissue is generated (inhomogeneously) only in a certain region of the domain. In order to focus on the effect of the sensing of compression on cell proliferation and extracellular matrix production and degradation, we assume that the behaviour of normal and abnormal cells differs only for the coefficients involving the sensing of stress. Therefore $\gamma_n = \gamma_a = \gamma$ and $\delta_n = \delta_a = \delta$. The non-dimensional model is then given by

$$\begin{cases} \dfrac{\partial n}{\partial \widetilde{t}} = \nabla \cdot (n \widetilde{\Sigma}'(\psi) \nabla \psi) + \left(H_\sigma(\psi - \psi_n) - \widetilde{\delta} \right) n\,, \\[2mm] \dfrac{\partial a}{\partial \widetilde{t}} = \nabla \cdot (a \widetilde{\Sigma}'(\psi) \nabla \psi) + \left(H_\sigma(\psi - \psi_a) - \widetilde{\delta} \right) a\,, \\[2mm] \dfrac{\partial m_n}{\partial \widetilde{t}} = \widetilde{\mu}_n n - \widetilde{\nu} \widetilde{c} m_n\,, \\[2mm] \dfrac{\partial m_a}{\partial \widetilde{t}} = \widetilde{\mu}_a a - \widetilde{\nu} \widetilde{c} m_a\,, \\[2mm] \dfrac{\partial \widetilde{c}}{\partial \widetilde{t}} = \widetilde{\kappa} \nabla^2 \widetilde{c} + \dfrac{1}{\widetilde{\tau}} (n + \widetilde{\pi}_a a - \widetilde{c})\,, \end{cases} \tag{45}$$
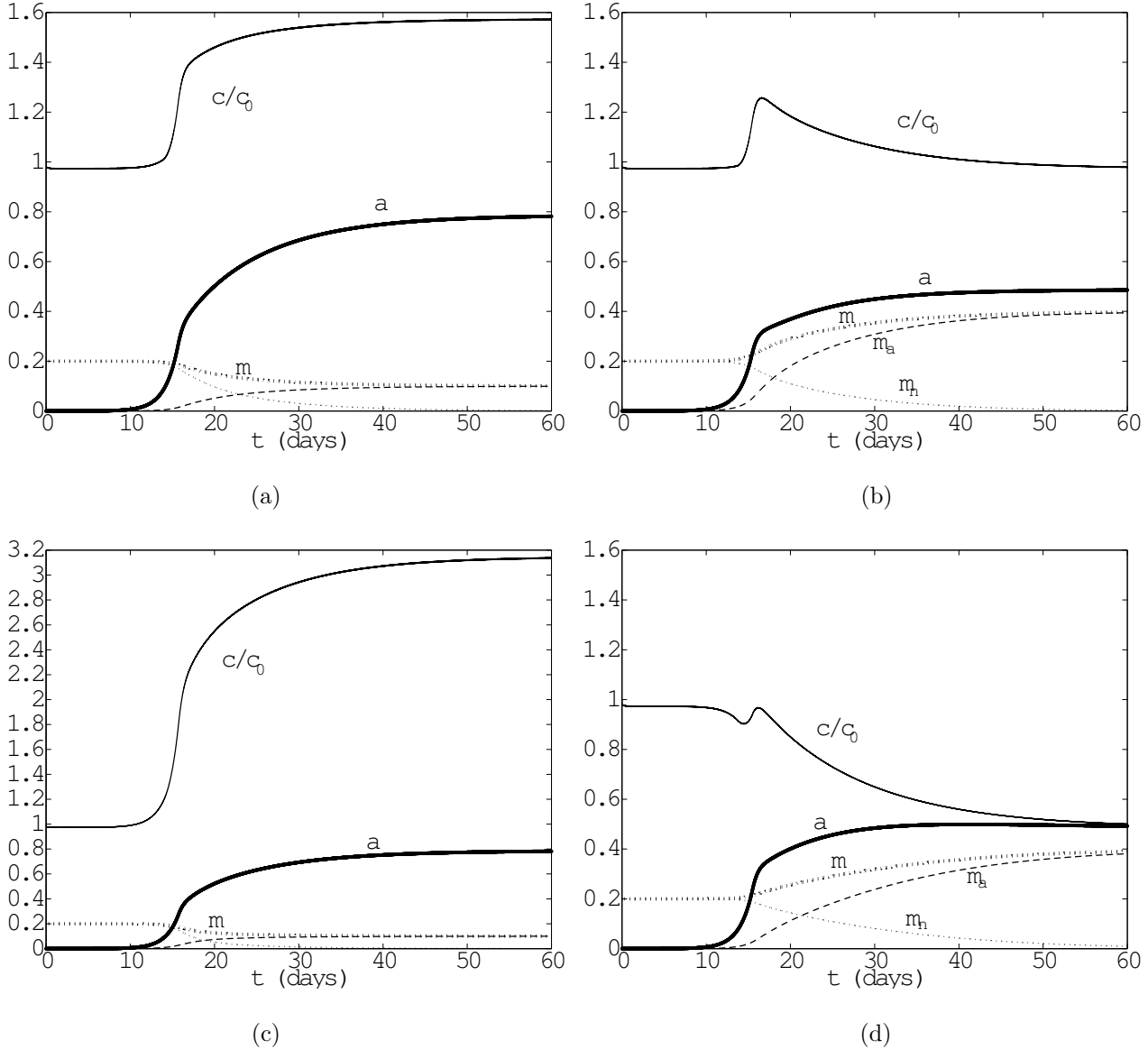
Figure 6: Hyperplasia with complete replacement of the tissue in the case of a pathological production of ECM and/or MDEs with respect to the situation in Figs. 4b and 5. In all Figs. full lines refer to scaled concentration of cells, thick full lines to the volume ratio of abnormal cells, dashed lines to the volume ratio of ECM produced by abnormal cells, doted lines to that produced by normal cells and thick dotted lines to their sum. The evolution of ψ and n is very similar to the one in Fig. 4b and is almost unaffected by the parameters used. In (a) $\mu_a = 0.05$ days^{-1}, in (b) $\mu_a = 0.2$ days^{-1}, in (c) $\pi_a/c_0 = 800$ days^{-1}, and in (d) $\pi_a/c_0 = 200$ days^{-1} with all other parameters as in Figs 4 and 5.

18

where

$$\tilde{t} = \gamma t, \qquad \tilde{\mathbf{x}} = \sqrt{\frac{\gamma}{KE}}\,\mathbf{x}\,, \qquad \widetilde{c} = \frac{c}{\pi_n \tau}\,. \tag{46}$$

and where

$$\widetilde{\mu}_i = \frac{\mu_i}{\gamma}\,, \qquad i = n, a\,,$$

$$\widetilde{\pi}_a = \frac{\pi_a}{\pi_n}\,, \qquad \widetilde{\tau} = \gamma\tau\,, \qquad \widetilde{\kappa} = \frac{\kappa}{KE}\,, \qquad \widetilde{\delta} = \frac{\delta}{\gamma}\,, \qquad \widetilde{\nu} = \frac{\nu \pi_n \tau}{\gamma}\,, \qquad \widetilde{\Sigma}'(\psi) = \frac{\Sigma'(\psi)}{E}\,. \tag{47}$$

We recall that n, a, m_n, and m_a are already dimensionless and observe that $\widetilde{\nu}/\widetilde{\mu}_n = M_n$ and $\widetilde{\nu}/\widetilde{\mu}_a = M_a$ defined in (20) and (44), respectively. We observe that measurements of K and E are not available in the literature, to our knowledge. However, from the fact that the order of magnitude of cell velocity is microns per hours and assuming a change of volume ratio of 0.1 over a cell diameter, we can argue that the order of magnitude of the product KE is 1 $\mu\mathrm{m}^2/\mathrm{s}$. Hence, the characteristic length in Eq.(46) is of the order of 100 μm and $\widetilde{\kappa}$ is of the order of 100.

The domain of integration in the following simulations is the entire space. However, when for numerical reasons we restrict to a finite domain zero-flux boundary conditions for the cells and the MDEs are imposed on the boundaries of the domain.

To start with we consider the spatially dependent version of the problem dealt with at the beginning of Section 4.3

$$\begin{cases} \dfrac{\partial n}{\partial \tilde{t}} = \nabla \cdot [n\widetilde{\Sigma}'(n+a)\nabla(n+a)] + [H_\sigma(n+a-\psi_n) - \widetilde{\delta}]n\,, \\[4mm] \dfrac{\partial a}{\partial \tilde{t}} = \nabla \cdot [a\widetilde{\Sigma}'(n+a)\nabla(n+a)] + [H_\sigma(n+a-\psi_a) - \widetilde{\delta}]a \end{cases} \tag{48}$$

with no-flux boundary conditions and the initial conditions $a(\tilde{t}=0,\tilde{x}) = a_0 \exp\{-\tilde{x}^2/2\sigma_0\}$ and $n(\tilde{t}=0,\tilde{x})$ such that the overall volume ratio corresponds to the homogeneous stationary configuration.

At the beginning, the same process occurring in the relaxed replacement phase (Phase I) occurs, with the abnormal population partially replacing the normal one (see Fig. 7), i.e.

$$a(\tilde{t},\tilde{x}) = a_0 e^{-\tilde{x}^2/2\sigma_0} e^{(1-\widetilde{\delta})\tilde{t}} \qquad \text{and} \qquad n(\tilde{t},\tilde{x}) = \psi_n - M_n - a(\tilde{t},\tilde{x})\,, \tag{49}$$

until

$$\tilde{t} \approx \frac{1}{1-\widetilde{\delta}}\log\frac{\widetilde{\delta}(\psi_n - M_n)}{a_0}\,, \tag{50}$$

for small σ. The simulation presented in Fig. 7 follows the estimate above. In fact, for the values of the parameters used Eq.(50) predicts that compression starts for $\tilde{t} > 4.1$ and coherently in Fig. 7c the line corresponding to $\tilde{t} = 5$ barely departs from the initial value. At this point in $\tilde{x} = 0$ compression starts and cells start moving away from the compressed regions. So Phase II and Phase III are different than in the spatially independent case treated in the previous sections. In the overcompressed regions where $\psi > \psi_n$ something like Phase II occurs with n exponentially decaying to zero and replaced by a. In the simulation the maximum overall compression characterising Phase III is achieved after about 40 (days, if $\gamma = 1$ days^{-1}), corresponding to a size of the hyperplasia which depends on $\sqrt{KE}$ and can be evaluated of the order of 1mm. This means that if the product of the permeability coefficient and the "Young's modulus" increases by two order of magnitude, i.e. for more permeable tissues and stiffly reacting cells, then the size needed to reach the overcompressed status increases by an order of magnitude. Of course, if growth is too slow with respect to motion, then the time needed to reach this phase increases further.

It is interesting to notice that, as observed experimentally, the growth of the hyperplasia is accompanied by a compression of the normal tissue near the interface separating the two tissues as shown by the peaks in Fig. 7a and qualitatively by the cartoon in Fig. 4a.

Recalling the characteristics of $H_\sigma(\phi)$ in (5) and in particular that it is non constant for $\phi \in [0,\sigma]$, in the hyperplasic tissue the solution tends to achieve an overall volume ratio in the interval $[\psi_a, \psi_a + \phi]$, while in the
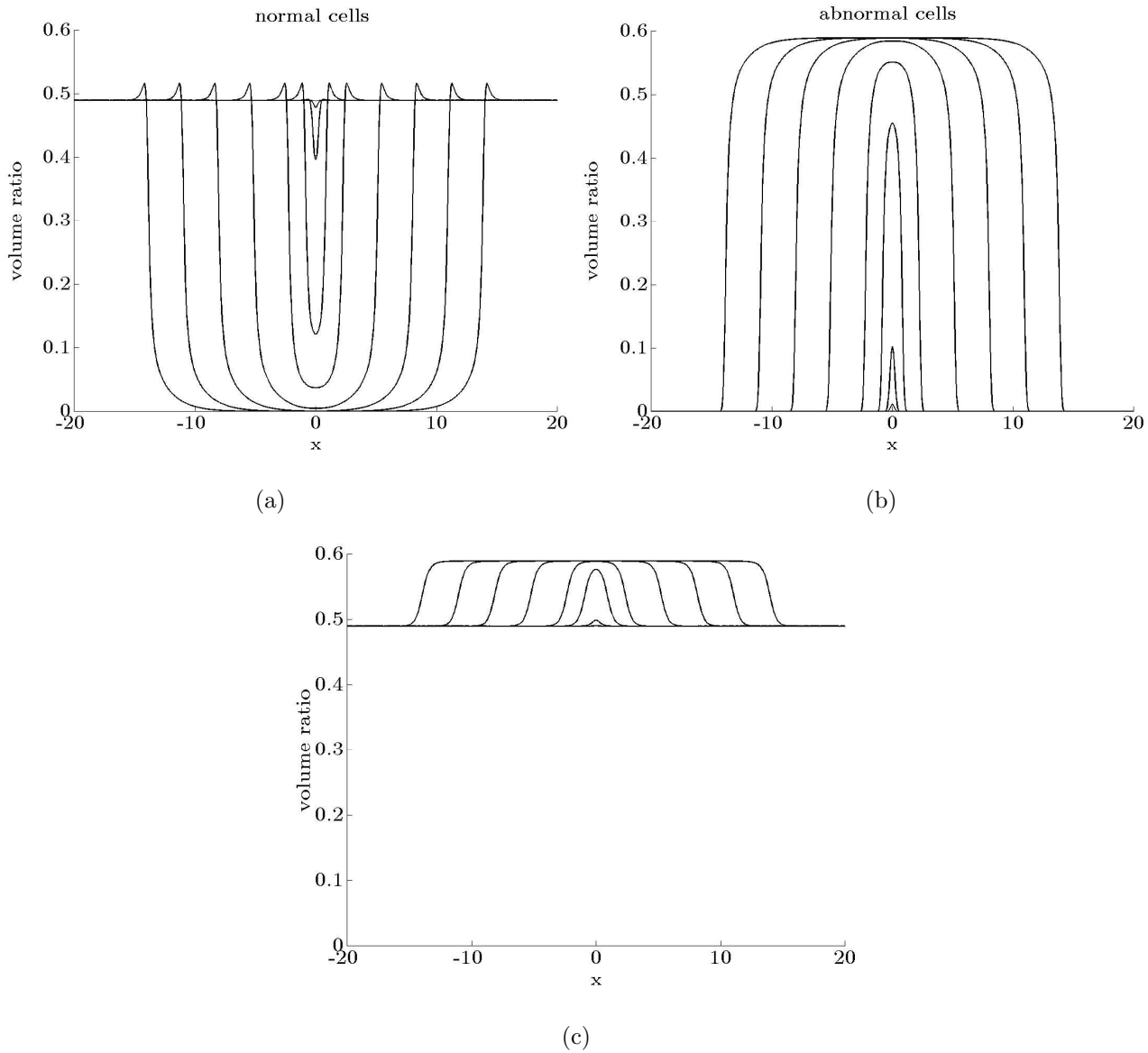
Figure 7: Tissue invasion for the following set of parameters $\widetilde{\delta} = 0.1$, $\psi_n = 0.6$, $\psi_a = 0.8$, $\sigma = 0.1$, $M_n = 0.2$, and at times $t = 0, 2.5, 5, 10, 20, 40, 60, 80$. At smaller times the dynamics follows the one described in Section 4.3. At larger times the travelling wave characteristic and the transition layer are evident. The compression of the normal tissue due to the expansion of the hyperplasia is also put in evidence by the peaks in (a) (see cartoon in Fig. 4a). In (c) the overall cell volume ratio $(n + a)$ at early times keeps its initial value following the relaxed replacement phase depicted in Fig. 4a.

normal tissue it tends to keep an overall volume ratio in the interval $[\psi_n, \psi_n + \phi]$. Actually, from the maximum principle $n + a + M_n \in [\psi_n, \psi_a + \phi]$ (see Fig. 7c).

This is true even if one starts from a segregated initial condition, i.e.

$$n(t = 0, \mathbf{x}) = 0 \quad \text{and} \quad a(t = 0, \mathbf{x}) \neq 0 \quad \text{in} \quad \Omega \,,$$

$$n(t = 0, \mathbf{x}) \neq 0 \quad \text{and} \quad a(t = 0, \mathbf{x}) = 0 \quad \text{in} \quad \mathbf{R}^3 - \Omega \,. \tag{51}$$

In this case, because of the degenerate character of the parabolic equations, the solution for a will always have compact support with a sharp front $\mathbf{x}_T(t)$ separating the two tissues. Coherently, the two populations move with the same velocity at the interface

$$\widetilde{\mathbf{v}} = -\mathbf{n} \cdot \nabla n = -\mathbf{n} \cdot \nabla a \quad \text{on} \quad \partial \Omega \,. \tag{52}$$

On the other hand, though the equation governing the evolution of $n + a$ is still degenerate parabolic, its solution is regular everywhere because the solution stays away from zero. In fact, in addition to (52), one has

$$n = a \,, \quad \text{on} \quad \partial \Omega \,. \tag{53}$$

This leads to the formation of a transition layer near the interface linking the solution with $n + a = a \in [\psi_a, \psi_a + \sigma]$ in the hyperplasic tissue and that with $n + a = n \in [\psi_n, \psi_n + \sigma]$ in the normal tissue.

In order to approximate such a solution and to identify the velocity of invasion of the hyperplasia we will look for a solution in the form of a travelling wave in the limit of small σ. Assuming $\widetilde{\psi}_a - \widetilde{\psi}_n \ll \widetilde{\psi}_n$ where, for instance, $\widetilde{\psi}_n = \psi_n - M_n$, and introducing the perturbations $\hat{n} = n - \widetilde{\psi}_n$ and $\hat{a} = a - \widetilde{\psi}_n$ one can write to leading order the following problem

$$\begin{cases} -\widetilde{v}\hat{a}' = \widetilde{\psi}_n \hat{a}'' + (1 - \widetilde{\delta})\widetilde{\psi}_n \,, & z < 0 \\[2mm] -\widetilde{v}\hat{n}' = \widetilde{\psi}_n \hat{n}'' - \widetilde{\delta}\widetilde{\psi}_n \,, & z > 0 \\[2mm] \hat{a} = \psi_a - \psi_n & \text{at} \ z = z_1 \,, \\[2mm] \hat{n} = 0 & \text{at} \ z = z_2 \,, \\[2mm] \hat{n} = \hat{a} \quad \text{and} \quad \hat{n}' = \hat{a}' = -\widetilde{v} & \text{at} \ z = 0 \,, \end{cases} \tag{54}$$

where the primes denote derivation with respect to $z = \widetilde{x} - \widetilde{v}\widetilde{t}$ and $\widetilde{v}$ is the velocity of the propagating front.

In order to identify z_1, z_2 we also assume

$$\begin{aligned} \hat{a}' = 0 & \quad \text{at} \quad z = \widetilde{z}_1 \,, \\ \hat{n}' = 0 & \quad \text{at} \quad z = z_2 \,. \end{aligned} \tag{55}$$

One then has

$$\hat{a} = \widetilde{\psi}_a - \widetilde{\psi}_n + \frac{(\widetilde{\delta} - 1)\widetilde{\psi}_n}{\widetilde{v}}(z - z_1) + \frac{(\widetilde{\delta} - 1)\widetilde{\psi}_n^2}{\widetilde{v}^2} \left\{ \exp\left[-\frac{\widetilde{v}(z - z_1)}{\widetilde{\psi}_n} \right] - 1 \right\} \quad \text{for } z \in [z_1, 0] \,,$$

$$\hat{n} = \frac{\widetilde{\delta}\widetilde{\psi}_n}{\widetilde{v}}(\widetilde{z} - z_2) + \frac{\widetilde{\delta}\widetilde{\psi}_n^2}{\widetilde{v}^2} \left\{ \exp\left[-\frac{\widetilde{v}(z - z_2)}{\widetilde{\psi}_n} \right] - 1 \right\} \quad \text{for } z \in [0, z_2] \,, \tag{56}$$

where

$$z_1 = \frac{\widetilde{\psi}_n}{\widetilde{v}} \ln\left(1 - \frac{\widetilde{v}^2}{\widetilde{\psi}_n(1 - \widetilde{\delta})} \right) \,,$$

$$z_2 = \frac{\widetilde{\psi}_n}{\widetilde{v}} \ln\left(1 + \frac{\widetilde{v}^2}{\widetilde{\psi}_n\widetilde{\delta}} \right) \,, \tag{57}$$
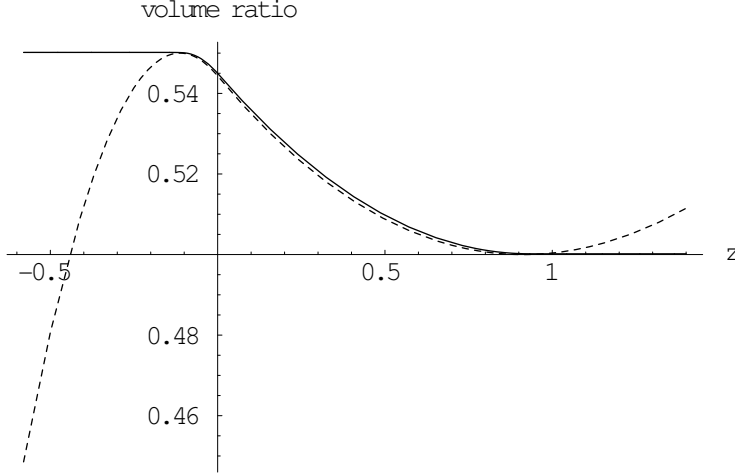
21

Figure 8: Travelling wave solution. Comparison between numerical (full line) and analytical results (dashed line) given by (56) for $\widetilde{\delta} = 0.1$, $\widetilde{\psi}_n = 0.5$ and $\widetilde{\psi}_a = 0.55$. $z = 0$ represents the moving interface between the normal and the abnormal tissue (on its right and left, respectively).

and the velocity of propagation is implicitly given by

$$\widetilde{\psi}_a - \widetilde{\psi}_n = -\frac{\widetilde{\psi}_n^2}{\widetilde{v}^2}\left[\widetilde{\delta}\ln\left(1 + \frac{\widetilde{v}^2}{\widetilde{\psi}_n\widetilde{\delta}}\right) + (1 - \widetilde{\delta})\ln\left(1 - \frac{\widetilde{v}^2}{\widetilde{\psi}_n(1 - \widetilde{\delta})}\right)\right]. \tag{58}$$

In the limit $\widetilde{v} \ll 1$, corresponding to $\psi_a \approx \psi_n$, one has the following approximations for the transition layer width

$$z_2 - z_1 \approx \sqrt{\frac{2(\psi_a - \psi_n)}{\widetilde{\delta}(1 - \widetilde{\delta})}}, \tag{59}$$

and for the velocity of propagation

$$\widetilde{v} \approx \sqrt{2\widetilde{\delta}(1 - \widetilde{\delta})(\psi_a - \psi_n)}, \tag{60}$$

which in dimensional form writes

$$v \approx \sqrt{2KE\delta\left(1 - \frac{\delta}{\gamma}\right)(\psi_a - \psi_n)}. \tag{61}$$

Fig. 8 shows a comparison between the travelling wave solution (56) and the one obtained numerically, while Fig. 9 compares the theoretical values of $\widetilde{v}$, z_1, z_2, and then of the transition layer thickness with the one obtained from the simulations.

The simulation presented in Fig. 10 instead refers to the numerical solution of the full system of PDEs (45). In this case the normal ECM is constantly digested and produced by the cells, but as the hyperplasic tissue is replacing the normal one, the abnormal ECM is now also replacing the normal one, as explained in the space independent case discussed in Section 3. Also in this case the travelling wave characteristic of the solution is evident. The evolution of the normal and abnormal cell populations are as in Fig. 7.

The concentration of MDEs increases because of the increase in the density of cells. Dynamics like the one discussed in Section 4.3 would be obtained for different values of the production rates of ECM by the two populations of cells, with the formation of an abnormal matrix which fills more space than normal.
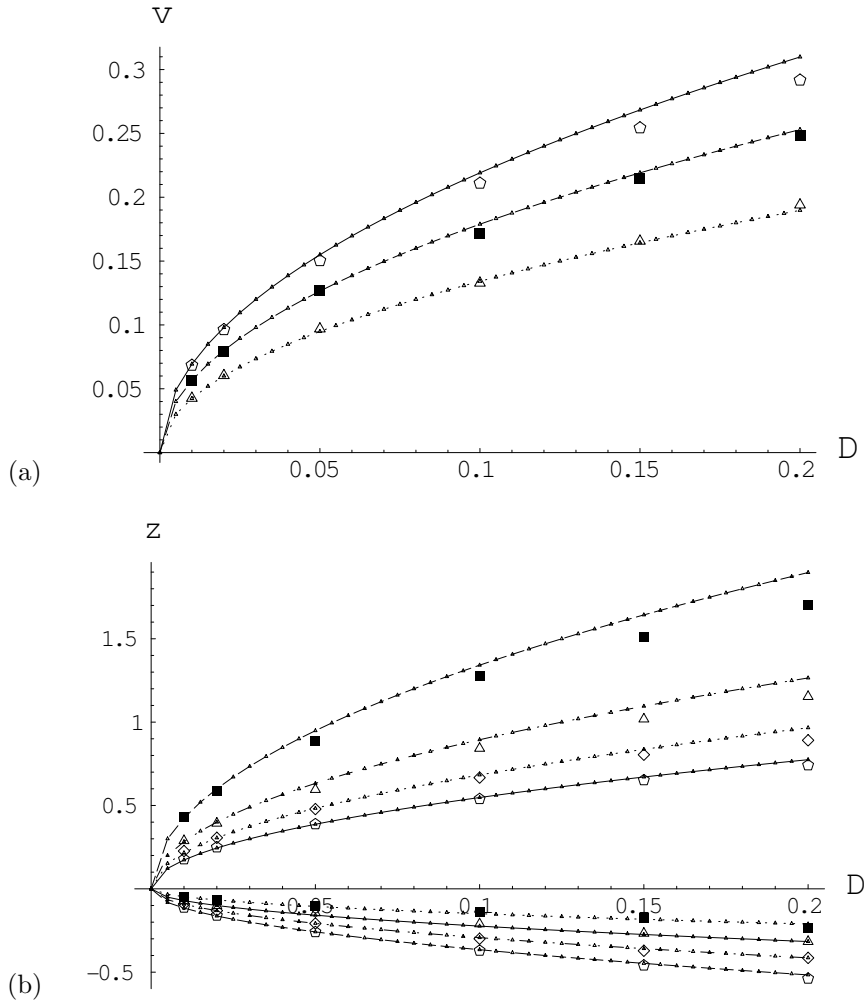
22

Figure 9: Travelling wave solution. (a) Velocity of propagation as a function of $D = \psi_a - \psi_n$ for $\widetilde{\delta} = 0.1, 0.2, 0.4$ (from lower to upper curve). (b) Transition layer thickness. The lower family of curves refer to z_1 and the upper family to z_2. The four curves refer to $\widetilde{\delta} = 0.1, 0.2, 0.3, 0.4$ from above to below in both cases. The thickness of the transition layer is then given by the distance between the two curves for given values of the parameters.
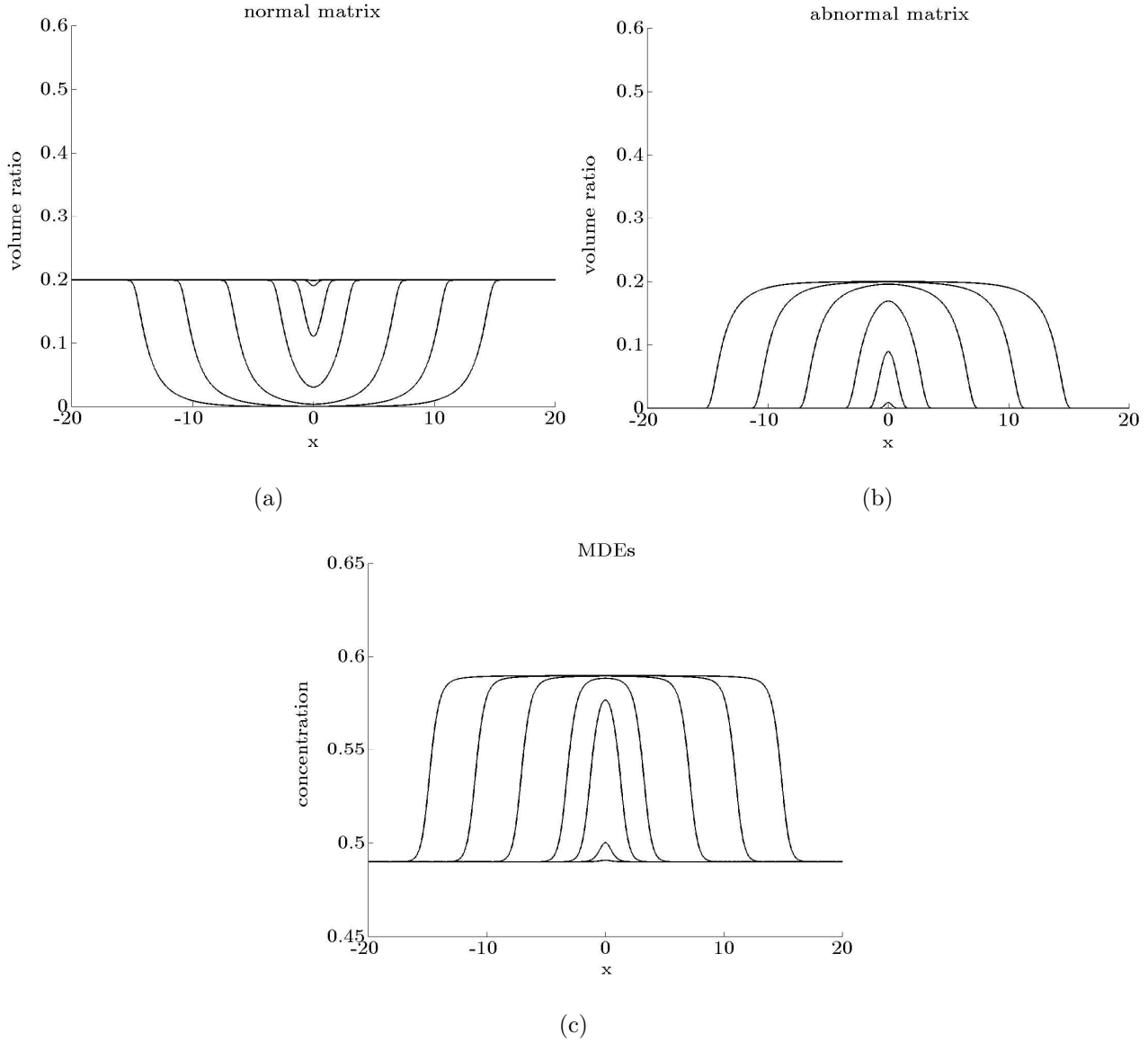
Figure 10: Tissue invasion with degradation and renewal of ECM through the constant production of MDEs. The evolution of the cell populations are similar to those in Fig. 7. The values of the parameters are the same as in Fig. 7 and $\widetilde{\pi}_a = 1$, $\widetilde{\mu}_n = \widetilde{\mu}_a = 0.1$, $\widetilde{\tau} = 0.005$, $\widetilde{\kappa} = 100$, $\widetilde{\nu} = 0.5$. The cleavage of normal ECM inside the hyperplasia and its substitution with the one produced by abnormal cells follows the front of the hyperplasia.

6 Discussion and Conclusions

In this paper we have presented and developed a mathematical model focussing on the potential role that an incorrect mechanotrasduction may play in causing the hyper-proliferation of cells in a tissue. In particular, we have shown how even a small loss of contact inhibition to growth and of compression responsiveness can represent by itself a clonal advantage which can give rise to the formation of hyperplasia and tumour growth. In replacing the normal tissue with the abnormal one, we have identified three phases which qualitatively correspond to the phenomenological description given by biologists: a first phase in which some abnormal cells simply replace the normal ones, a second phase in which the hyper-proliferation of the abnormal cells causes a progressive compression within the tissue itself, and a third phase in which the tissue reaches a compressed state, which presses on the surrounding environment. The difference in the ability to stand the compressed state leads to a progressive invasion of the surrounding tissue.

At the same time, because of the constant remodelling of the extracellular matrix, the components produced by the tumour cells progressively replace those previously present. In the case in which the production rates or the release of matrix degrading enzymes is different than those corresponding to the physiological state, the model foresees the formation of a tissue characterized by a pathological percentage of ECM, as observed in many tumours and illness. For instance, an increased production of extracellular matrix not balanced by an increased release of matrix degrading enzymes leads to tissues with more extracellular matrix than normal, as in many fibrosis and in colon and prostate cancers. On the other hand, excessive degradation of extracellular matrix due to excessive production of matrix degrading enzymes leads to tissues with less extracellular matrix than normal, as in other malignant tumours and many other cronic inflammatory diseases.

From a travelling wave analysis exploiting the fact that usually there is only a slight incorrect sensing of the compression level, we obtained an estimate of the velocity of growth of the hyperplasia which is proportional to $\sqrt{\psi_a - \psi_n}$, i.e. to the square root of the difference of the volume ratios at which abnormal and normal cells stop duplicating by contact inhibition. Therefore, as expected, smaller disfunctions lead to slower invasions of the sorrounding healthy tissue. Throughout the paper the role of nutrients and growth factors was neglected, though we are well aware of their importance, and that even the switching on and off of the duplication process is mediated by growth promoting and inhibitory factors, through the activation of suitable protein cascades.

In this respect, it would be interesting to develop a multiscale model which takes into account in full of the cascade of events recalled in Fig. 2 possibly joined with those involving growth factors. Of course, in order to do that one needs to have estimates on the affinity constants. In absence of such measurements, one could initially start with a Boolean reasoning, which leads for instance to the assumption that a chronic cadherin underexpression leads to uncontrolled growth at any compression level (i.e., $\psi_a = 1$ in (15)).

Another interesting generalization of the model would be to take into account of the fact that the remodelling process is strongly affected by the stresses and strains the tissue is subject to. Of course, in order to do that quantitative measurement of the dependence of the production of ECM and MDEs from stress and/or strain would be needed. Quantitative measurements on the growth rates and on the production rates of ECM and MDEs under different conditions would also allow a further validation of the model presented here.

Acknowledgements

References

[1] J.A. Adam and N. Bellomo, Eds. (1996). **A Survey of Models on Tumour Immune Systems Dynamics**, (Birkhäuser, Boston).

[2] M. Alini and G.A. Losa (1991). Partial characterization of proteoglycans isolated from neoplastic and nonneoplastic human breast tissues, *Cancer Res.* **51**: 1443–1447.

[3] D. Ambrosi and F. Guana (2004). Stress modulated growth, *Quart. J. Mech. Appl. Math.*, in press.

[4] D. Ambrosi and F. Mollica (2002). On the mechanics of a growing tumour, *Int. J. Engng. Sci.* **40**: 1297–1316.

[5] D. Ambrosi and F. Mollica (2003). Mechanical models in tumour growth, in **Cancer Modelling and Simulation**, L. Preziosi Ed., (Chapman & Hall/CRC Press), 121–145.

[6] D. Ambrosi and F. Mollica (2004). The role of stress in the growth of a multicell spheroid, *J. Math. Biol.* **48**: 477-499.

[7] D. Ambrosi and L. Preziosi (2002). On the closure of mass balance models for tumour growth, *Math. Mod. Meth. Appl. Sci.* **12**: 737–754.

[8] A.R.A. Anderson, M.A.J. Chaplain, R.J. Steele, E.L. Newman, and A. Thompson (2000). Mathematical modelling of tumour invasion and metastasis, *J. Theor. Medicine* **2**: 129–154.

[9] R.P. Araujo and D.L.S. McElwain, (2004). A hystory of the study of solid tumour growth: The contribution of mathematical modelling, *Bull. Math. Biol.* **66**: 1039–1091.

[10] N. Barker and H. Clevers (2000). Catenins, wnt signalling and cancer, *Bioessays* **22**: 961–965.

[11] K.F. Becker, M.J. Atkinson, U. Reich, I. Becker, H. Nekarda, J.R. Siewert, and H. Hofler (1994). E-cadherin gene mutation provide clues to diffuse gastric carcinoma, *Cancer Res.* **54**: 3845–3852.

[12] N. Bellomo and E. De Angelis, Eds. (2003). Modeling and simulation of tumour development, treatment, and control, *Math. Comp. Modeling* **37**: 1121–1252.

[13] N. Bellomo, E. De Angelis, and L. Preziosi, L. (2003). Multiscale modeling and mathematical problems related to tumour evolution and medical therapy, *J. Theor. Medicine* **5**, 111–136.

[14] D.A. Berk, F. Yuan, M. Leunig, and R.K. Jain (1993). Fluorescence photobleaching with spatial Fourier analysis: measurement of diffusion in light scattering media, *Biophys. J.* **65**: 2428–2436.

[15] M. Bertsch, M.E. Gurtin, D. Hilhorst, and L.A. Peletier (1985). On interacting populations that disperse to avoid crowding: Preservation and segregation, *J. Math. Biol.* **23**: 1–13.

[16] E.C. Breen (2000). Mechanical strain increases type I collagen expression in pulmonary fibroblasts in vitro, *J. Appl. Physiol.* **88**: 203–209.

[17] C.J.W. Breward, H.M. Byrne, and C.E. Lewis (2001). Modeling the interactions between tumour cells and a blood vessel in a microenvironment within a vascular tumour, *Eur. J. Appl. Math.* **12**: 529–556.

[18] C.J.W. Breward, H.M. Byrne, and C.E. Lewis (2002). The role of cell-cell interactions in a two-phase model for avascular tumour growth, *J. Math. Biol.* **45**: 125–152.

[19] C.J.W. Breward, H.M. Byrne, and C.E. Lewis (2003). A multiphase model describing vascular tumour growth, *Bull. Math. Biol.* **65**: 609–640.

[20] C.E. Brewster, P.H. Howarth, R. Djukanovic, J. Wilson, S.T. Holgate, and W.R. Roche (1990). Myofibroblasts and subepithelial fibrosis in bronchial asthma, *Am. J. Respir. Cell Mol. Biol.* **3**: 507–511.

[21] L.F. Brown, A.J. Guidi, S.J. Schnitt, L. van de Water, M.L. Iruela-Arispe, T.-K. Yeo, K. Tognazzi, and H.F. Dvorak (1999). Vascular stroma formation in carcinoma in situ, invasive carcinoma and metastatic carcinoma of the breast, *Clin. Cancer Res.* **5**: 1041–1056.

[22] H.M. Byrne, J.R. King, D.L.S. McElwain, and L. Preziosi, (2003). A two-phase model of solid tumour growth, *Appl. Math. Letters* **16**: 567–573.

[23] H.M. Byrne and L. Preziosi (2004). Modeling solid tumour growth using the theory of mixtures, *Math. Med. Biol.* **20**: 341–366.

[24] S.B. Carter (1965). Principles of cell motility: The direction of cell movement and cancer invasion, *Nature* **208**: 1183–1187.

[25] M.A. Castilla, M.V.A. Arroyo, E. Aceituno, P. Aragoncillo, F. R. Gonzalez-Pacheco, E.Texeiro, R. Bragado, and C. Caramelo (1999). Disruption of cadherin-related junctions triggers autocrine expression of vascular endothelial growth factor in bovine aortic endothelial cells. Effect on cell proliferation and death resistance, *Circ. Res.* **85**: 1132–1138.

[26] U. Cavallaro, B. Schaffhauser, and G. Christofori (2002). Cadherin and the tumour progression: Is it all in a switch?, *Cancer Lett.* **176**: 123–128.

[27] L. Caveda, I. Martin-Padura, P. Navarro, F. Breviario, M. Corada, D. Gulino, M.G. Lampugnani, and E. Dejana (1996). Inhibition of cultured cell growth by vascular endothelial cadherin (cadherin-5/VE-cadherin), *J. Clin. Invest.* **98**: 886–893.

[28] A.F. Chambers and L.M. Matrisian (1997). Changing views of the role of matrix metalloproteinases in metastasis, *J. Natl. Cancer Inst.* **89**: 1260–1270.

[29] M.A.J. Chaplain, Ed. (1999). Special Issue *Math. Mod. Methods Appl. Sci.* **9**.

[30] M.A.J. Chaplain, Ed. (2002). Special Issue on Mathematical Modeling and Simulations of Aspects of Cancer Growth, *J. Theor. Medicine* **4**.

[31] M.A.J. Chaplain and A.R.A. Anderson (2003). Mathematical modeling of tissue invasion, in **Cancer Modelling and Simulation**, L. Preziosi Ed., (Chapman & Hall/CRC Press), 264–297.

[32] M. Chiquet (1999). Regulation of extracellular matrix gene expression by mechanical stress, *Matrix Biol.* **18**: 417–426.

[33] M. Chiquet, M. Matthisson, M. Koch, M. Tannheimer, and R. Chiquet-Ehrismann (1996). Regulation of extracellular matrix synthesis by mechanical stress, *Biochem. Cell Biol.* **74**: 737–744.

[34] M. Chiquet, A.S. Renedo, F. Huber, and M. Flück (2003). How do fibroblasts translate mechanical signals into changes in extracellular matrix production?, *Matrix Biol.* **22**: 73–80.

[35] L. Christensen (1992). The distribution of fibronectin, laminin and tetranectin in human breast cancer with special attention to the extracellular matrix, *APMIS Suppl.* **26**: 1–39.

[36] G. Christofori and H. Semb (1999). The role of cell-adhesion molecule E-cadherin as a tumors-suppressor gene, *Trends Biochem. Sci.* **24**: 73–76.

[37] C.J. Chuong and Y.C. Fung (1986). On residual stresses in arteries, *ASME J. Biomech. Eng.* **108**: 189–192.

[38] S. Coats, W.M. Flanagan, J. Nourse, and J. Roberts (1996). Requirement of p27kip1 for restriction point control of the fibroblast cell cycle, *Science* **272**: 877–880.

[39] D.E. Coplen, E.J. Macarak, and P.S. Howard (2003). Matrix synthesis by bladder smooth muscle cells is modulated by stretch frequency, *In Vitro Cell. Dev. Biol.* **39**: 157–162.

[40] E. De Angelis and L. Preziosi (2000). Advection-diffusion models for solid tumours *in vivo* and related free-boundary problems, *Math. Mod. Meth. Appl. Sci.* **10**: 379–408.

[41] E. Dejana, M.G. Lampugnani, M. Giorgi, M. Gaboli, and P.C. Marchisio (1990). Fibrinogen induces endothelial cell adhesion and spreading via the release of endogenous matrix proteins and the recruitment of more than one integrin receptor, *Blood* **75**: 1509–1517.

[42] L. Deleu, F. Fuks, D. Spitkovsky, R. Hörlein, S. Faisst, and J. Rommelaere (1998). Opposite transcriptional effects of cyclic AMP-responsive elements in confluent or p27kip-overexpressing cells versus serum-starved or growing cells, *Molec. Cell. Biol.* **18**: 409–419.

[43] A. Di Carlo and S. Quiligotti (2002). Growth and balance, *Mech. Res. Comm.* **29**: 449–456.

[44] C. Dietrich, K. Wallenfrang, F. Oesch, and R. Wieser (1997). Differences in the mechanisms of growth control in contact-inhibited and serum-deprived human fibroblasts, *Oncogene* **15**: 2743–2747.

[45] S.J. Franks and J.R. King (2003). Interactions between a uniformly proliferating tumour and its surrounding. Uniform material properties, *Math. Med. Biol.* **20**: 47–89.

[46] J.P. Freyer and R.M. Sutherland (1986). Regulation of growth saturation and development of necrosis in EMT6/Ro multicellular spheroids by the glucose and oxygen supply, *Cancer Res.* **46**: 3504–3512.

[47] Y.C. Fung (1993). **Biomechanics: Mechanical Properties of Living Tissues**, (Springer-Verlag, New York).

[48] L. Fusi, A. Farina, and D. Ambrosi (2004). Mathematical modelling of a solid-liquid mixture with mass exchange between constituents, *Math. Mech. Solids*, in press.

[49] U. Gat, R. DasGupta, L. Degenstein, and E. Fuchs (1998). De novo hair follicle morphogenesis and hair tumors in mice expressing a truncated β-catenin in skin, *Cell* **95**: 605–614.

[50] R.A. Gatenby and E.T. Gawlinski (1996). A reaction–diffusion model of cancer invasion, *Cancer Research* **56**: 5745–5753.

[51] S.J. George and A. Dwivedi (2004). MMPs, cadherins, and cell proliferation, *Trends Cardiovasc. Mech.* **14**: 100–105.

[52] C.J. Gottardi, E. Wong, and B.M. Gumbiner (2001). E-cadherin suppresses cellular transformation by inhibiting β-catenin signalling in an adhesion-independent manner, *J. Cell. Biol.* **153**: 1049–1060.

[53] M.E. Gurtin and R.C. McCamy (1977). On the diffusion of biological populations, *Math. Biosci.* **33**: 35–49.

[54] D. Hanahan and J. Folkman (1996). Patterns and emerging mechanisms of the angiogenic switch during tumorigenesis, *Cell* **86**: 353–364.

[55] N. Harada, Y. Tamai, T. Ishikawa, G. Sauer, K. Takaku, M. Oshima, and M.M. Taketo (1999). Intestinal polyposis in mice with a dominant stable mutation of the β-catenin gene, *EMBO J.* **18**: 5931–5942.

[56] K.M. Harja and E.R. Fearon (2002). Cadherin and catenin alterations in human cancer, *Genes Chromosomes Cancer* **34**: 255–268.

[57] G. Helmlinger, P.A. Netti P.A., H.C. Lichtenbeld, R.J. Melder and R.K. Jain (1997). Solid stress inhibits the growth of multicellular tumour spheroids, *Nature Biotech.* **15**: 778–783.

[58] L. Hengst, V. Dulic, J.M. Slingerland, E. Lees, and S.I. Reed (1994). A cell cycle-regulated inhibitor of cyclin-dependent kinase, *Proc. Natl. Acad. Sci. USA* **91**: 5291–5295.

[59] L. Hengst and S.I. Reed (1996). Translational control of p27Kip1 accumulation during the cell cycle, *Science* **271**: 1861–1864.

[60] T. Hillen (2002). Hyperbolic models for chemosensitive movement, *Math. Mod. Meth. Appl. Sci.* **12**: 1007–1034.

[61] J.D. Humphrey and K.R. Rajagopal (2002). A constrained mixture model for growth and remodeling of soft tissues, *Math. Mod. Meth. Appl. Sci.* **12**: 407–430.

[62] M. Hutton, F. Willenbrock, K. Brocklehurst, and G. Murphy (1998). Kinetic analysis of the mechanism of interaction of full-length TIMP-2 and gelatinase A: Evidence for the existence of a low affinity intermediate, *Biochemistry* **37**: 10094–10098.

[63] P.R.A. Johnson (2001). Role of human airway smooth muscle in altered extracellular matrix production in asthma, *Clin. Exp. Pharm. Physiol.* **28**: 233–236.

[64] E.D. Karagiannis and A.S. Popel (2004). A theoretical model of type I collagen proteolysis by matrix metalloproteinases (MMP)2 and membrane type 1 MMP in the presence of tissue inhibitor of metalloproteinases 2, *J. Biol. Chem.* **279**: 39105–39114.

[65] A. Kato, H. Takahashi, Y. Takahashi, and H. Matsushime (1997). Inactivation of the cyclin D-dependent kinase in the rat fibroblast cell line, 3Y1, induced by contact inhibition, *J. Biol. Chem.* **272**: 8065–8070.

[66] S.-G. Kim, T. Akaike, T. Sasagawa, Y. Atomi, and H. Kurosawa (2002). Gene expression of type I and type III collagen by mechanical stretch in anterior cruciate ligament cells, *Cell Struct. Funct.* **27**: 139–144.

[67] M. Kjaer (2004). Role of extracellular matrix in adaptation of tendons and skeletal muscle to mechanical loading, *Physiol. Rev.* **84**: 649–698.

[68] J. Klominek, K.H. Robert, and K.-G. Sundqvist (1993). Chemotaxis and haptotaxis of human malignant mesothelioma cells: Effects of fibronectin, laminin, type IV collagen, and an autocrine motility factor–like substance, *Cancer Res.* **53**: 4376–4382.

[69] J. Lacovara, E.B. Cramer, and J.P. Quigley (1984). Fibronectin enhancement of directed migration of B16 melanoma cells, *Cancer Res.* **44**: 1657–1663.

[70] R. Lagace, J.A. Grimaud, W. Schurch, and T.A. Seemayer (1985). Myofibroblastic stromal reaction in carcinoma of the breast: Variations of collagenous matrix and structural glycoproteins, *Vircows Arch. A, Pathol. Anat. Histopathol.* **408**: 49–59.

[71] J.A. Lawrence and P.S. Steeg (1996). Mechanisms of tumour invasion and metastasis, *World J. Urol.* **14**: 124–130.

[72] C.H. Lee, H.J. Shin, I.H. Cho, Y.-M. Kang, I.A. Kim, K.-D. Park, and J.-W. Shin (2005). Nanofiber alignment and direction of mechanical strain affect the ECM production of human ACL fibroblant, *Biomaterials* **26**: 1261–1270.

[73] S. Levenberg, A. Yarden, Z. Kam, and B. Geiger (1999). p27 is involved in N-cadherin-mediated contact inhibition of cell growth and S-phase entry, *Oncogene* **18**: 869–876.

[74] J.R. Levick (1987). Flow through interstitium and other fibrous matrices, *Q. J. Cogn. Med. Sci.* **72**: 409–438.

[75] L.A. Liotta and E.C. Kohn (2001). The microenvironment of the tumor-host interface, *Nature* **411**: 375–379.

[76] D. MacKenna, S.R. Summerour, and F.J. Villarreal (2000). Role of mechanical factors inmodulatin cardiac fibroblast function and extracellular matrix synthesis, *Cardiovasc. Res.* **46**: 257–263.

[77] J.J. Mao and H.-D. Nah (2004). Growth and development: Hereditary and mechanical modulations, *Amer. J. Orthod. Dentofac. Orthop.* **125**: 676–689.

[78] M. Marotta, R. Vecchione, G. Martino, F.P. Darmiento, M. De Cesare, and P. Rosati (1985). Glycosaminoglycan-enriched extracellular matrix surrounds intraductal carcinoma of human breast, histochemical study, *Appl. Pathol.* **3**: 179–185.

[79] L.M. Matrisian (1992). The matrix–degrading metalloproteinases, *Bioessays* **14**: 455–463.

[80] J.B. McCarthy and L.T. Furcht (1984). Laminin and fibronectin promote the directed migration of B16 melanoma cells in vitro, *J. Cell Biol.* **98**: 1474–1480.

[81] C.M. Nelson and C.S. Chen (2003). VE-cadherin simultaneously stimulates ad inhibits cell proliferation by altering cytoskeletal structure and tension, *J. Cell Science* **116**: 3571–3581.

[82] A.C. Newby and A.B. Zaltsman (2000). Molecular mechanisms in intimal hyperplasia, *J. Pathol.* **190**: 300–309.

[83] T. Oda, Y. Kanai, T. Okama, K. Yoshiura, Y. Shimoyama, W. Birchmeier, T. Sugimura, and S. Hirohashi (1994) E-cadherin gene mutation in human gastric carcinoma cell lines, *Proc. Natl. Acad. Sci. USA* **91**: 1858–1862.

[84] J. Ottl, D. Gabriel, G. Murphy, V. Knauper, Y. Tominaga, H. Nagase, M. Kroger, H. Tschesche, W. Bode, and L. Moroder (2000). Recognition and catabolism of synthetic heterotrimetric collagen peptides by matrix metalloproteinases, *Chem. Biol.* **7**: 119–132.

[85] K. Painter and T. Hillen (2002). Volume filling and quorum-sensing in models for chemosensitive movement, *Can. Appl. Math. Quart.* **10**: 501–543.

[86] S.L. Parson, S.A. Watson, P.D. Brown, H.M. Collins, and R.J.C. Steele (1997). Matrix metalloproteinases, *Brit. J. Surg.* **84**: 160–166.

[87] A.J. Perumpanani and H.M. Byrne (1996) Biological inferences from a mathematical model of malignant invasion, *Invasion and Metastases* **16**: 209–221.

[88] K. Polyak, J. Kato, M.J. Solomon, C.J. Sherr, J. Massague, J.M. Roberts, and A. Koff (1994). p27Kip1, a cyclin-Cdk inhibitor, links transforming growth factor-β and contact inhibition to cell cycle arrest, *Genes & Develop.* **8**: 9–22.

[89] K. Polyak, M.H. Lee, H. Erdjument-Bromage, A. Koff, J.M. Roberts, P. Tempst, and J. Massague (1994). Cloning of p27Kip1, a cyclic-dependent kinase inhibitor and a potential mediator of extracellular antimitogenic signals, *Cell* **78**: 59–66.

[90] L. Preziosi, Ed. (2003). **Cancer Modelling and Simulation**, (CRC-Press - Chapman Hall, Boca Raton).

[91] L. Preziosi and L. Graziano (2003). Multiphase models of tumour growth: General framework and particular cases, **Mathematical Modeling and Computer in Biology and Medicine**, Proceeedings of the 5th Conference on the ESMTB, (Società Editrice Esculapio), 622–628.

[92] P. Pujuguet, A. Hammann, M. Moutet, J. L. Samuel, F. Martin, and M. Martin (1996). Expression of fibronectin EDA+ and EDB+ isoforms by human and experimental colorectal cancer, *Am. J. Patho.* **148**: 579–592.

[93] J.P. Quigley, J. Lacovara, and E.B. Cramer (1983). The directed migration of B–16 melanoma–cells in response to a haptotactic chemotactic gradient of fibronectin, *J. Cell Biol.* **97**: A450–451.

[94] I.J. Rao, J.D. Humphrey, and K.R. Rajagopal (2003). Biological growth and remodeling: A uniaxial example with possible application to tendons and ligaments, *CMES* **4**: 439–455.

[95] J.I. Risinger, A. Berchuck, M.F. Kohler, and J. Boyd (1994). Mutation of E-cadherin gene in human gynecological cancers, *Nature Genetics* **7**: 98–102.

[96] E. Rouslahti (1997) Stretching is good for a cell, *Science* **276**: 1345–1346.

[97] B. Rubinfeld, B. Souza, I. Albert, O. Muller, S.H. Chamberlain, F.R. Masiark, S. Munemitsu, and P. Polakis (1993). Association of the APC gene product with β-catenin. *Science* **262**: 1731–1734.

[98] R. Skalak, S. Zargaryan, R.K. Jain, P.A. Netti, and A. Hoger, (1996). Compatibility and genesis of residual stress by volumetric growth, *J. Math. Biol.* **34**: 889–914.

[99] B. St. Croix, C. Sheehan, J.W. Rak, V.A. Florenes, J.M. Slingerland, and R.S. Kerbel (1998). E-cadherin-dependent growth suppression is mediated by the cyclin-dependent kinase inhibitor p27(Kip1), *J. Cell Biol.* **142**: 557–571.

[100] W.G. Stetler-Stevenson, R. Hewitt, and M. Corcoran (1996). Matrix metallo–proteinases and tumour invasion: From correlation to causality to the clinic, *Cancer Biol.* **7**: 147–154.

[101] A. Stockinger, A. Eger, J. Wolf, H. Beug, and R. Foisner (2001). E-cadherin regulates cell growth by modulating proliferation-dependent β-catenin transcriptional activity, *J. Cell. Biol.* **152**: 1185–1196.

[102] L.K. Su, B. Vogelstein, and K.W. Kinzel (1993). Association of the APC tumor suppressor gene with catenins, *Science* **262**: 1734–1737.

[103] R.M. Sutherland and R.E. Durand (1984) Growth and cellular characteristics of multicell spheroids, *Recent Results in Cancer Research* **95**: 24–49.

[104] L. Taber and J.D. Humphrey (2001). Stress–modulated growth, residual stress and vascular heterogeneity, *ASME J. Biomech. Eng.* **123**: 528–535.

[105] T. Takeuchi, A. Misaki, S.-B. Liang, A. Tachibana, N. Hayashi, H. Sonobe, and Ohtsuki Y. (2000). Expression of T-cadherin (CDH13, H-cadherin) in human brain and its characteristics as a negative growth regulator of epidermal growth factor in neuroblastoma cells, *J. Neurochem.* **74**: 1489–1497.

[106] J. Takeuchi, M. Sobue, E. Sato, M. Shamoto, and K. Miura (1976). Variation in glycosaminoglycan components of breast tumours, *Cancer Res.* **36**: 2133–2139.

[107] Y. Tzukatani, K. Suzuki, and K. Takahashi (1997). Loss of density-dependent growth inhibition and dissociation of α-catenin from E-cadherin, *J. Cell. Physiol.* **173**: 54–63.

[108] S. Tzukita, M. Itoh, A. Nagafuchi, S. Yonemura, and S. Tsukita (1993). Submembrane junctional plaque proteins include potential tumor suppressor molecules, *J. Cell Biol.* **123**: 1049–1053.

[109] E.B. Uglow, G.D. Angelini, and S.J. George (2000). Cadherin expression is altered during intimal thickening in humal sapphenous vein, *J. Submicrosc. Cytol. Pathol.* **32**: C113–C119.

[110] E.B. Uglow, S. Slater, G.B. Sala-Newby, C.M. Aguilera-Garcia, G.D. Angelini, A.C. Newby, and S.J. George (2003). Dismantling of cadherin-mediated cell-cell contacts modulates smooth muscle cell proliferation, *Circ. Res.* **92**: 1314–1321.

[111] P. Vijayagopal, J.E. Figueroa, and E.A. Levine (1998). Altered composition and increased endothelial cell proliferative activity of proteoglycans isolated from breast carcinoma, *J. Surg. Oncol.* **68**: 250–254.

[112] M.E. Warchol (2002). Cell proliferation and N-cadherin interactions regulate cell proliferation in the sensory epithelia of the inner ear, *J. Neurosci.* **22**: 2607–2616.

[113] J. Winston, F. Dong, and W.J. Pledger (1996). Differential modulation of G1 cyclins and the Cdk inhibitor p27kip1 by platelet-derived growth factor and plasma factors in density-arrested fibroblasts, *J. Biol. Chem.* **271**: 11253–11260.

[114] K. Wolf, R. Mueller, S. Borgmann, E.-B. Broecker, and P. Friedl (2003). Ameboid shape change and contact guidance: T-lymphocyte crawling through fibrillar collagen is independent of matrix remodelling by MMPs and other proteases, *Blood* **102**: 3262–3269.

[115] C.-M. Yang, C.-S. Chien, C.-C. Yao, L.-D. Hsiao, Y.-C. Huang, and C.B. Wu (2004). Mechanical strain induces collagenases-3 (MMP-13) expression in MC3T3-E1 osteoblastic cells, *J. Biol. Chemistry* **279**: 22158–22165.

[116] Y. Zhang, S. Nojima, H. Nakayama, J. Yulan, and H. Enza (2003). Characteristics of normal stromal components and their correlation with cancer occurrence in human prostate, *Oncol. Rep.* **10**: 207–211.